Geochimica et Cosmochimica Acta Vol. 55, pp. 601–619

0016-7037/91/$3.00 + .00

Composition of chondrule silicates in LL3-5 chondrites and implications for their nebular history and parent body metamorphism

TIMOTHY J. MCCOY,[1,2] EDWARD R. D. SCOTT,[1] RHIAN H. JONES,[2] KLAUS KEIL,[1] and G. JEFFREY TAYLOR[1]

[1]Planetary Geosciences Division, Department of Geology and Geophysics, School of Ocean and Earth Science and Technology, University of Hawaii, Honolulu, HI 96822, USA

[2]Institute of Meteoritics, Department of Geology, University of New Mexico, Albuquerque, NM 87131, USA

(*Received April* 26, 1990; *accepted in revised form November* 20, 1990)

Abstract—Our petrologic studies of 75 type IA and type II porphyritic olivine chondrules in nine selected LL group chondrites of type 3.3 to type 5 and comparisons with published studies of chondrules in Semarkona (LL3.0) show that compositions of silicates and bulk chondrules, but not overall chondrule textures, vary systematically with the petrologic type of the chondrite. These compositional trends are due to diffusive exchange between chondrule silicates and other phases (e.g., matrix), such as those now preserved in Semarkona, during which olivines in both chondrule types gained Fe^{2+} and Mn^{2+} and lost Mg^{2+}, Cr^{3+}, and Ca^{2+}. In a given LL4-5 chondrite, the olivines from the two chondrule types are identical in composition. Enrichments of Fe^{2+} in olivine are particularly noticeable in type IA chondrules from type 3.3–3.6 chondrites, especially near grain edges, chondrule rims, grain boundaries, and what appear to be annealed cracks. Compositional changes in low-Ca pyroxene lag behind those in coexisting olivine, consistent with its lower diffusion rates. With increasing petrologic type, low-Ca pyroxenes in type IA chondrules become enriched in Fe^{2+} and Mn^{2+} and depleted in Mg^{2+}, Cr^{3+}, and Al^{3+}. These compositional changes are entirely consistent with mineral equilibration in chondritic material during metamorphism. From these compositional data alone we cannot exclude the possibility that chondritic material was metamorphosed to some degree in the nebula, but we see no evidence favoring nebula over asteroidal metamorphism, nor evidence that the chondrule reacted with nebular gases after crystallization. Modelling of the equilibration of chondrule olivines suggests that heterogeneous FeO concentrations in olivine could be preserved after cooling from 600°C at rates of 1–10°C/Ma for at least tens to hundreds of millions of years. This is consistent with published estimates for the maximum metamorphic temperatures in type 3 chondrites, thermal histories derived from metallographic and fission-track cooling rates, and 4.4 Ga ^{40}Ar-^{39}Ar ages for ordinary chondrites. Since the lifetime of the solar nebula was not more than 10^6 years and there is abundant evidence that meteorite parent bodies were heated, some even above their melting point, we confidently conclude that the formation of type 3.3–5 ordinary chondrites from type 3.0 material by metamorphism occurred in parental asteroids, not the solar nebula.

INTRODUCTION

BECAUSE OF THE COMPLEXITY of chondrites and the lack of progress in characterizing conditions during their formation and evolution, there are considerable disagreements concerning the thermal histories of chondrites in the solar nebula and on parent bodies and the relative importance of various heat sources that may have operated in these environments. The conventional view, at least for ordinary chondrites, is that chondrules formed as a result of melting of pre-existing solids by unidentified heat sources in the solar nebula (TAYLOR et al., 1983; GROSSMAN, 1988) and that chondrites were metamorphosed in planetesimals as a result of heating by electrical induction or ^{26}Al decay (MCSWEEN et al., 1988). Most authors believe that the mineralogical and textural differences between type 3–6 ordinary chondrites result largely from asteroidal metamorphism of material that resembled type 3 chondrites (VAN SCHMUS and WOOD, 1967; DODD, 1969; HUSS et al., 1981; LUX et al., 1980; SEARS and HASAN, 1987). In particular, these authors conclude that the composition of homogeneous silicates in chondrules of type 4–6 chondrites was established by equilibration of heterogeneous silicates in chondrules and matrix of type 3 chondrites.

Some authors disagree with the conventional view and argue that nebular processes were important in modifying the properties of chondrules and other chondritic components after they formed (see HEWINS, 1989). KURAT (1988) argues that the composition of mineral grains in ordinary chondrites results solely from exchange between grains and nebular gases and not from any asteroidal processing. For CV3 carbonaceous chondrites, PECK and WOOD (1987) and HUA et al. (1988) argue similarly that fayalite-rich rims on forsterite-rich chondrules and FeO enrichments in chondrule interiors are the result of nebular condensation and exchange.

An entirely different view is that of REID and FREDRIKSSON (1967) and FREDRIKSSON (1983) who conclude that diverse crystallization histories, not metamorphism, are responsible for the homogeneity of chondrule silicates in types 4–6 and their heterogeneity in type 3 chondrites. In support of their views, these authors argue that grain growth occurs more rapidly than silicate homogenization and that friable chondrites with homogeneous silicates such as Bjurböle could not have formed from a heterogeneous type 3 precursor by metamorphism. FREDRIKSSON (1983) argues further that silicates with unequilibrated compositions are common in ordinary type 4–6 chondrites and that these meteorites are not meta-

morphic rocks. SCOTT et al. (1985) agree that these chondrites are breccias, but they argue that the components experienced diverse parent body metamorphic histories. Detailed petrologic studies of ordinary chondrites of type 3–6 are needed to resolve these issues.

Although much information about the thermal history of chondrites has been deduced from studies of compositional zoning in grains of metallic Fe,Ni (WOOD, 1967; WILLIS and GOLDSTEIN, 1981a, 1983), less progress has been made from analogous studies of silicate zoning in chondrules. This is partly because diffusion rates in silicates at low temperatures are known to lower accuracy than those for Fe-Ni diffusion in metal. A more fundamental difference, however, is that zoning in chondrule silicates probably results from both igneous and metamorphic processes (DODD, 1969), whereas zoning in metal grains, at least in unshocked chondrites, is entirely metamorphic in origin. This is because any igneous zoning in metal grains in unshocked chondrites was erased during slow cooling; Ni heterogeneities in taenite developed during kamacite growth below 600°C (WILLIS and GOLDSTEIN, 1981b). Characteristics of chondrule silicates that result from igneous and metamorphic processing must be distinguished carefully before precise models can be developed to explain silicate zoning.

Previous studies of the compositions of chondrule silicates have mostly been comparative studies of the bulk properties of chondrules in chondrites of diverse petrologic type (DODD et al., 1967; LUX et al., 1980). Until recently, the only detailed study of zoning in chondrules was by MIYAMOTO et al. (1986). These authors analyzed chondrule silicates in two type 3.6–3.7 ordinary chondrites and modelled their thermal histories during chondrule solidification and subsequent metamorphism. However, these authors were not able to clearly distinguish the effects of solidification and metamorphism, and the two chondrites that they studied, Allan Hills A77278 and A77299, appear to be breccias containing materials that were metamorphosed to diverse degrees (SCOTT, 1984; HEWINS, 1990).

We have studied type IA and type II porphyritic olivine chondrules (MCSWEEN, 1977; SCOTT and TAYLOR, 1983) in LL group chondrites of type 3.3–5 to distinguish igneous and metamorphic features and to constrain their thermal histories. We chose types IA and II chondrules because of their widespread occurrence and our ability to identify them using textural, not compositional, criteria. Type IA chondrules are characterized by round shapes and small, euhedral olivines. Fe,Ni metal and troilite are present in variable amounts and may cause an irregular chondrule shape when present in large amounts (>10 vol%). Low-Ca pyroxene crystals commonly rim the chondrule and may poikilitically enclose olivine; in some chondrules, low-Ca pyroxenes have rims of Ca-rich pyroxene. Type II chondrules have large (30–250 μm), euhedral olivines, lack pyroxene phenocrysts, and have large (500–1000 μm) apparent diameters and irregular shapes.

We have compared the compositions of olivines, pyroxenes, mesostases, and bulk chondrules in LL3.3–5 chondrites with corresponding compositional data for types IA and II chondrules in the Semarkona (LL3.0) chondrite (JONES and SCOTT, 1989; JONES, 1990). Silicate compositions in the Semarkona chondrules are largely consistent with closed-system fractional crystallization. Because H3.0 and L3.0 chondrites are not known (SEARS and HASAN, 1987), we have only studied LL chondrites in this work. However, analogous studies of types IA and II chondrules in CO3 chondrites (SCOTT and JONES, 1990) suggest that our conclusions may be applicable to other chondrite groups. We conclude in this paper that porphyritic olivine chondrules in LL3.3–5 chondrites were derived from chondrules like those in Semarkona by metamorphic equilibration of chondritic material. The time scales for metamorphism are too long for nebular processing, but are consistent with heating in asteroidal bodies.

SAMPLES AND TECHNIQUES

Table 1 lists the section numbers and sources of the nine LL chondrites we studied. Our data for chondrule silicates in two LL4 chondrites, Kelly and Soko-Banja, and two LL5 chondrites, Tuxtuac and Krahenberg, are not presented here, as the compositions of their chondrules are almost identical to those of Sevilla (LL4) and Olivenza (LL5), except for very minor differences in FeO.

Parnallee (LL3.6) was selected because a preliminary survey identified it as one of relatively few type 3 ordinary chondrites in which the chondrules appear to have had similar metamorphic histories (SCOTT et al., 1983; SCOTT, 1984). In addition, chondrule silicates in Parnallee are roughly midway in composition between those in Semarkona (LL3.0) and the equilibrated LL chondrites. Lastly, Parnallee does not appear to have experienced sufficient shock reheating to alter mineral compositions. Allan Hills A81251 (hereafter ALH A81251) was selected because its subtype of 3.3 is intermediate between those of Semarkona and Parnallee. A survey of five LL4 chondrites found only one, Bo Xian, with homogeneous olivines and heterogeneous pyroxenes. No LL6 chondrites were studied, because of the difficulty in identifying types IA and II chondrules.

Scanning electron microscopy and wavelength dispersive analysis of olivines, pyroxenes, and mesostases were performed on a JEOL 733 microprobe, operated at an accelerating potential of 15 kV, a beam current of 20 nA, and counting times of up to 40 s. Typical detection limits (wt%) for individual analyses of minor elements are: TiO_2, 0.02; Al_2O_3, 0.04; Cr_2O_3, 0.03; MnO, 0.04; CaO, 0.04; P_2O_5, 0.05; and Na_2O, 0.05. Differential matrix effects were corrected using the method of BENCE and ALBEE (1968).

Both large and small grains of olivine and pyroxene were analyzed in each chondrule. For chondrules with heterogeneous olivines, 5 to 37 point analyses were made at both grain edges and cores in both interiors and edges of chondrules. For chondrules with homogeneous olivines, 3 to 5 olivine analyses were made. In type IA chondrules, 5 to 15 analyses were also made on low-Ca pyroxene, measuring both grain edges and cores. Zoning profiles were measured at intervals of 2–10 μm across 3 to 9 olivine and pyroxene grains of diverse sizes in each of 12 chondrules in Parnallee. Errors of individual analyses within the zoning profiles are approximately 1.0% of amount present for concentrations greater than 1.0 wt% and approximately 10% on concentrations less than 1.0 wt%.

Fe,Ni metal and bulk chondrule compositions were measured on an ARL EMX-SM microprobe at an accelerating potential of 15 kV and a beam current of about 20 nA. Counting times of 10 s were used on standards and samples. Fe,Ni metal compositions were corrected using standard ZAF procedures. For the determination of metallographic cooling rates, taenite grains lightly etched with a dilute solution of nitric acid in alcohol were measured. Only equant grains with radially symmetric etching patterns were included. Taenite radii were measured with a calibrated eyepiece to an accuracy of ± 1 μm.

Bulk compositions of chondrules were measured using a broad beam (40–100 μm) and corrected using the methods of LUX et al. (1980), as modified by JONES and SCOTT (1989). Since our primary interest was in the compositional changes in the silicate portions of chondrules, we avoided Fe,Ni metal and troilite during probe analysis. The abundances of these phases were determined by modal analysis (e.g., KEIL, 1962).

Table 1. Classification and sources of LL-group chondrites and number of chondrules studied.

Meteorite	Pet. Type*	Section Numbers	Source†	Chondrule Prefix‡	No. of Type IA	No. of Type II
ALH A81251	3.3	14	MWG	None	5	4
Parnallee	3.6	1110-1	USNM	None	6	6
Bo Xian	4	265	UCLA	None	3	2
		266		A	2	3
		267		B	3	0
		268		C	0	2
Sevilla	4	841	UNM	None	3	3
		846		A	3	1
Kelly	4	515	UNM	None	1	2
Soko-Banja	4	3078-1	USNM	None	1	3
		3078-2		A	2	2
Olivenza	5	796	UNM	None	3	2
		797		A	2	2
Tuxtuac	5	627	UNM	None	2	2
Krahenberg	5	394	UNM	None	1	1
		396		A	1	2

* Classification from GRAHAM *et al.* (1985) except for type 3 chondrites from SEARS and HASAN (1987) and Sevilla from CASANOVA *et al.* (1990).

† Sources: MWG, Meteorite Working Group; UCLA, Univ. of California at Los Angeles; UNM, Univ. of New Mexico; USNM, Smithsonian Institution, U.S. National Museum of Natural History.

‡ Prefixes used in tables 4,5,7 and 8 to identify thin section.

We note that substitution of Fe for Mg in olivines and low-Ca pyroxenes in the compositional range appropriate for chondrites can cause changes of up to 15% relative in the concentrations of other oxides. The compositional changes that we discuss are much larger than this and are not caused by Fe-Mg substitution.

RESULTS

Type IA Chondrules

Type IA chondrules were selected following the procedure of JONES and SCOTT (1989) using only petrographic, not compositional, criteria, in an effort to match the subset of type IA chondrules studied by them in Semarkona. Petrographic properties of type IA chondrules in the nine type 3.0–5 LL chondrites are identical (Fig. 1) except for the degree of devitrification or grain size of the mesostasis, which increases with petrologic type.

Compositional differences between olivines in type IA chondrules from type 3.0–5 chondrites are summarized in Table 2, which shows the mean olivine compositions in each of six LL chondrites. For each chondrite, the mean composition was derived by averaging the mean values for each of 5 to 15 chondrules; standard deviations of the means are also given in Table 2. Mean compositions and standard deviations for each of the 30 chondrules in LL3.3–5 chondrites are given by MCCOY (1990). Concentrations of FeO and MnO increase through the type 3.0–5 sequence, whereas CaO, Al_2O_3, Cr_2O_3, and TiO_2 decrease.

Mean fayalite and CaO concentrations in olivine grains in the 45 type IA chondrules are shown in Fig. 2. Bars show the standard deviations of the 5 to 37 analyses made on each chondrule. Chondrules in Parnallee (LL3.6) typically have the widest ranges of fayalite and CaO concentrations: e.g., Fa, 5–26 mol%; CaO, 0.02–0.2 wt%. Chondrules in the type 4–6 ordinary chondrites show the smallest ranges: e.g., Fa, 27.6–28.2; CaO, <0.02–0.03 wt%. Figure 2 shows that the ranges of fayalite and CaO concentrations in individual chondrules in the type 3.0–5 sequence are entirely consistent with the conversion of type 3.0 olivine compositions into type 4–5 compositions by the addition of Fe^{2+} and loss of Mg^{2+} and Ca^{2+}.

In Figs. 3 and 4 we compare zoning profiles from rim to core across olivine grains in four type IA chondrules in Parnallee with analogous profiles for Semarkona chondrules from JONES and SCOTT (1989). Figure 3 shows that olivines in Parnallee chondrules have core-to-rim enrichments of FeO and MnO and depletions of CaO. These are consistent with the addition of Fe^{2+} and Mn^{2+} and loss of Mg^{2+} and Ca^{2+} that are necessary to convert type 3.0 to type 4 olivines.

Whereas the Parnallee profiles shown in Fig. 3a–c are typical, those for Cr_2O_3 and Al_2O_3 in Fig. 4a and b are not. Most olivine crystals do not show significant trends in Cr_2O_3 concentrations, but some crystals have enrichments at their rims (Fig. 4a). Chromium concentrations in Parnallee olivines should tend to decrease from core to rim if chromium diffuses out of type 3.0 olivines during conversion to type 4 material, as suggested by mean olivine compositions (Table 2). The observed increase may be inherited, and not completely erased from, the type 3.0 material, as some Semarkona chondrules show fourfold increases in their Cr_2O_3 concentrations near the olivine rim. Al_2O_3 concentrations in olivines are mostly below detection limit (0.04 wt%) but a few crystals are enriched at their rims. The expected trend for Al_2O_3 in Parnallee olivines (a decrease from core to rim) may also be masked by strong and heterogeneous enrichments of Al_2O_3

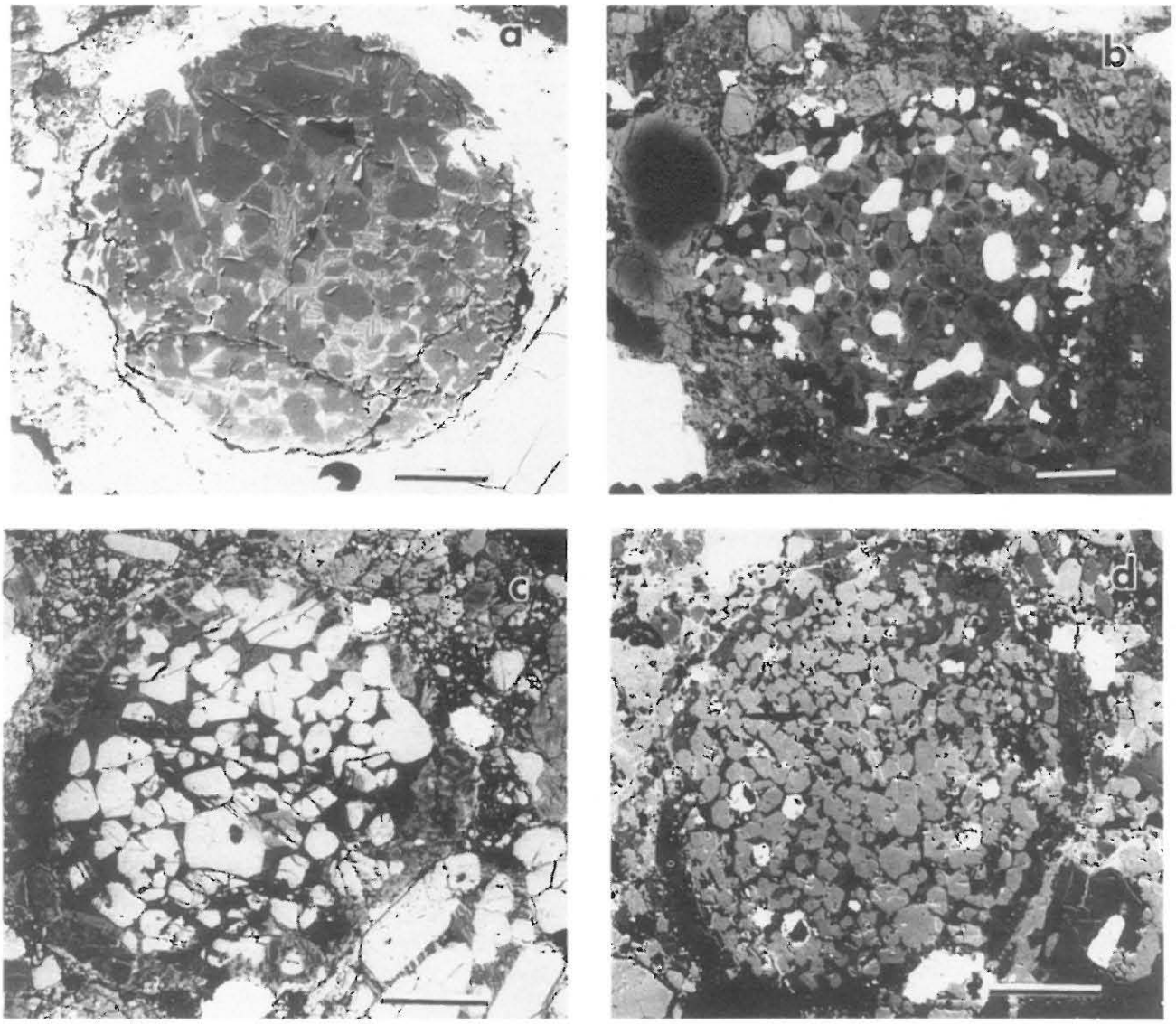

FIG. 1. Back-scattered electron images of representative type IA chondrules in four LL chondrites: (a) Semarkona, type 3.0; (b) Parnallee, type 3.6; (c) Bo Xian, type 4; and (d) Kelly, type 4. Despite their drastically different olivine compositions, the chondrules are very similar in texture, indicating that their thermal histories during crystallization were similar. The mean compositions of olivine and pyroxene grains and the standard deviation of the analyses are as follows: (a) Fal.1 ± 0.2, Fs1.8 ± 0.3; (b) Fa20 ± 2, Fs3 ± 2; (c) Fa29 ± 0.2, Fs7 ± 4; (d) Fa27 ± 0.3, Fs23 ± 0.6. The systematic increase in the FeO concentrations of olivines and pyroxenes through the type 3–4 sequence results from the exchange of Fe^{2+} and Mg^{2+} between type IA chondrule silicates and those in other chondrules and the matrix. Olivines in (c) are whiter than those in (d) largely because of enhanced contrast. Large olivine outside chondrule in (b) has zoning similar to some olivines inside the chondrule, indicating that chondrule mesostasis is not a significant barrier to diffusion. Scale bars = 100 μm.

near the rims of many olivines in several type IA chondrules in Semarkona (Fig. 4b; JONES and SCOTT, 1989).

The Fe-Mg zoning of olivines in type IA chondrules in Parnallee is clearly shown in back-scattered electron images (Figs. 1b and 5). FeO enrichments are visible in olivine grains near chondrule rims and also in the rims of grains in the central region of the chondrules. In addition, Fig. 5 shows that FeO is enriched along grain boundaries between olivines and along linear or curvilinear features within olivine crystals that we interpret as pre-existing cracks. Some of the curvilinear FeO enrichments contain phases relatively high in Cr_2O_3 and Al_2O_3 but too small for quantitative microprobe analysis. We interpret the grain boundaries and crack-like features to be high-diffusivity paths during metamorphism. For a given chondrule in type 3.3–4 chondrites, no compositional differences were detected between olivines enclosed in pyroxene and those surrounded by mesostasis, at a similar distance from the chondrule rim.

Analytical data for low-Ca pyroxenes in 31 type IA chondrules that contain appreciable modal pyroxene are given in

Table 2. Mean compositions (wt. %) of olivines in type IA chondrules in LL3.0-5 chondrites.

Meteorite	Type	SiO_2	TiO_2	Al_2O_3	Cr_2O_3	FeO	MnO	MgO	CaO	Total	Fa	N*
Semarkona	3.0	42.1	0.04	0.14	0.37	1.0	0.09	55.7	0.31	99.75	1.0	15
		0.3	*0.02*	*0.09*	*0.25*	*0.5*	*0.05*	*1.3*	*0.12*		*0.5*	
ALH A81251	3.3	41.3	0.04	0.10	0.17	3.7	0.08	53.4	0.21	99.00	3.8	5
		0.6	*0.02*	*0.06*	*0.08*	*1.6*	*0.07*	*1.4*	*0.13*		*1.6*	
Parnallee	3.6	39.1	0.02	0.04	0.04	15.7	0.23	44.7	0.16	99.99	16.5	6
		0.7	*0.01*	*0.01*	*0.01*	*3.8*	*0.09*	*2.8*	*0.07*		*4.3*	
Bo Xian	4	37.3	0.04	<0.04	0.02	25.4	0.43	37.2	<0.04	100.43	28.0	8
		0.7	*0.03*		*0.01*	*1.7*	*0.03*	*1.3*			*2.0*	
Sevilla	4	37.9	0.03	<0.04	0.03	25.8	0.45	37.0	<0.04	101.24	28.0	6
		0.2	*0.01*		*0.02*	*0.2*	*0.01*	*0.6*			*0.4*	
Olivenza	5	37.8	0.02	<0.04	0.04	27.4	0.44	35.5	0.04	101.25	30.0	5
		0.1	*0.01*		*0.01*	*0.1*	*0.01*	*0.3*	*0.01*		*0.2*	

* Number of chondrules analyzed.
Italicized figures are standard deviations of the mean compositions of individual chondrules.
Sources: Semarkona, JONES and SCOTT (1989); higher petrologic types, this work.

Table 3 and plotted in Figs. 6–8 using procedures identical to those chosen for olivine compositional data. Table 3 shows that mean FeO and MnO concentrations in low-Ca pyroxene increase from type 3.0 to type 5 and Cr_2O_3 and Al_2O_3 decrease, as they do for olivine; TiO_2 and CaO show no trends. The absence of a CaO trend appears inconsistent with the increase

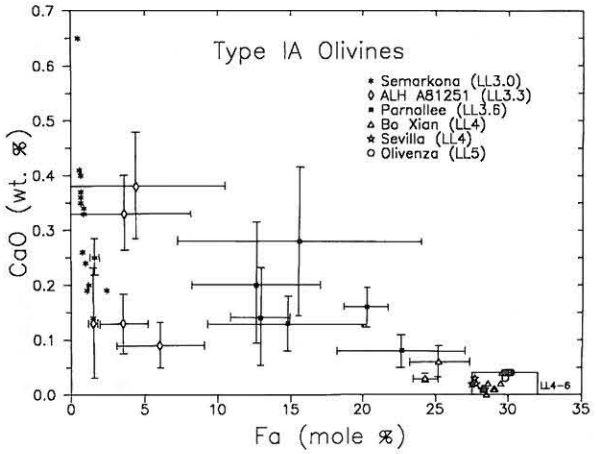

FIG. 2. Mean concentrations of fayalite and CaO in olivine grains from 45 type IA chondrules in six LL3.0–5 chondrites. The bars indicate one standard deviation of 5 to 37 analyses in each chondrule; they are omitted for all but two of the chondrules in the type 4–5 chondrites, because they are comparable in size or smaller than the plotted symbols, and for all but one of the Semarkona chondrules because of their narrow compositional range. Although some overlap exists between the fayalite concentration ranges of chondrules from different chondrites, mean fayalite concentrations for individual chondrules increase with little overlap through the petrologic sequence. CaO concentrations show more overlap, but the mean concentrations for chondrites decrease through this sequence. These compositional trends and the decrease in olivine heterogeneity through the sequence are consistent with the conversion of type 3.0 material to type 3.3–5 by metamorphism. Changes in FeO probably reflect equilibration between FeO-poor type IA olivines and FeO-rich olivines in the matrix and other chondrules, whereas CaO changes may reflect exchange between olivine and pyroxene. The Semarkona data are from JONES and SCOTT (1989) and the ranges in LL4–6 chondrites are from GOMES and KEIL (1980) (Fa) and this work (CaO).

in the CaO concentration of low-Ca pyroxene with increasing petrologic type observed by HEYSE (1978) and SCOTT et al. (1986) in LL chondrites. However, these authors analyzed randomly selected points from all occurrences of low-Ca pyroxene. In this study, we have concentrated on type IA chondrules, where low-Ca pyroxenes are often rimmed by high-Ca pyroxene. Furthermore, the boundary between low-Ca and high-Ca pyroxene is often gradational. This could result in excessive analyses of Ca-enriched pyroxene in this study, especially in Semarkona (JONES and SCOTT, 1989).

Figure 6 shows the variation in the mean fayalite and ferrosilite concentrations in coexisting olivine and low-Ca pyroxene in type IA chondrules through the LL3.0–5 sequence. Mean compositions for type 3.3, type 3.6, and Bo Xian chondrules define a curved path from the type 3.0 region near the origin (Fa, 0.6–2.4; Fs, 1.0–3.5) to the LL4–6 box (Fa, 27–32; Fs, 23–26). For chondrules in the type 3.3 chondrite, fayalite concentrations are much more heterogeneous than ferrosilite concentrations, whereas for Bo Xian we found the opposite. The curved path of mean compositions in Fig. 6 and the change in the relative degree of heterogeneity in olivine and low-Ca pyroxene are entirely consistent with the conversion by metamorphism of type 3.0 to type 4–5 material, as Fe-Mg diffusion is much faster in olivine than in low-Ca pyroxene (e.g., HUEBNER and NORD, 1981).

A plot of ferrosilite against Cr_2O_3 concentrations in the low-Ca pyroxene of type IA chondrules (Fig. 7) also shows a trend from LL3.0 chondrites, which have high Cr_2O_3 concentrations, to LL5–6 chondrites with low concentrations. Zoning profiles for FeO across low-Ca pyroxene grains in type IA chondrules from Parnallee (Fig. 8) are also compatible with derivation of pyroxene compositions in chondrites of petrologic type 5–6 from those in type 3.0. For example, low-Ca pyroxenes in Semarkona (LL3.0) have low FeO and are essentially unzoned; those of intermediate type (e.g., Parnallee, LL3.6) have slightly elevated FeO contents in their cores and show drastic increases at their borders; and those in higher petrologic grades (e.g., Sevilla, LL4) have high FeO and are homogeneous (Fig. 8). In Bo Xian (LL4), pronounced Fe-Mg heterogeneities in low-Ca pyroxene (Fig. 9) and very

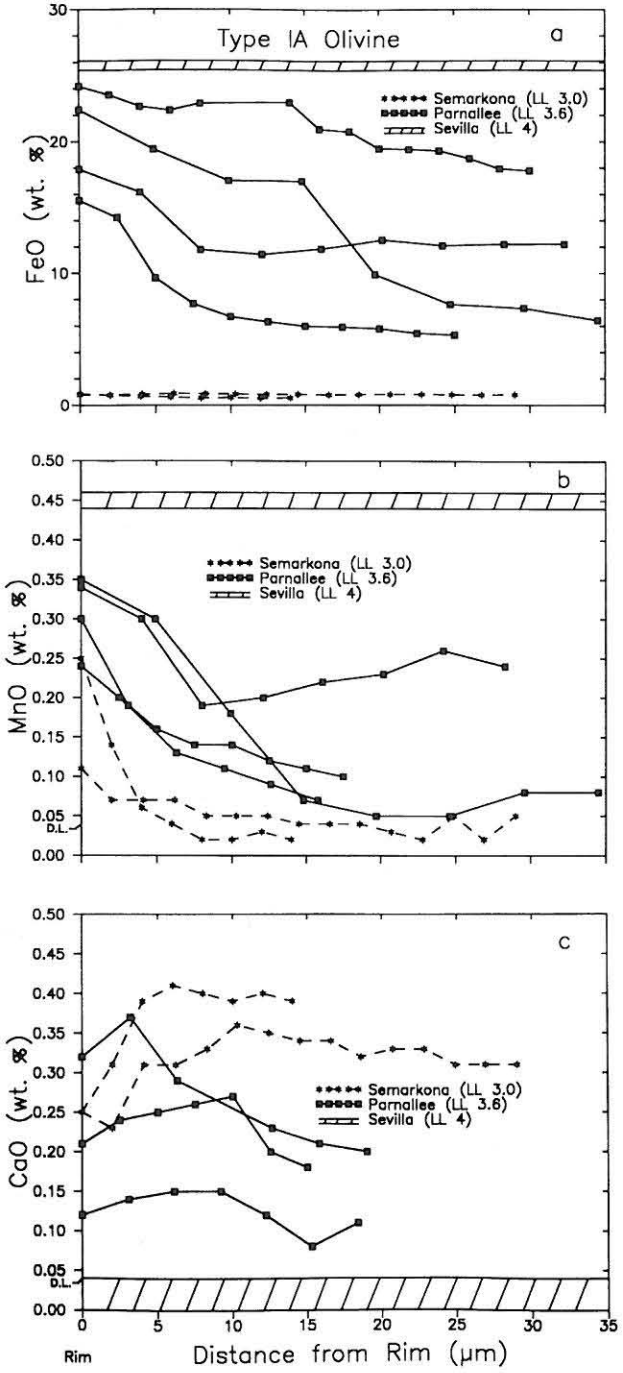

FIG. 3. Comparison of typical zoning profiles from rim to core of olivine grains in type IA chondrules in Parnallee (LL3.6), analogous profiles from Semarkona (LL3.0) (JONES and SCOTT, 1989), and the total range shown by olivines in type IA chondrules from Sevilla (LL4): (a) FeO, (b) MnO, and (c) CaO. Although olivine compositions in Parnallee chondrules partially overlap those in the type 3.0 and 4 chondrites, mean FeO and MnO concentrations increase from type 3.0 to 4, whereas CaO concentrations decrease. FeO and MnO concentrations in Parnallee decrease from rim to core of the olivine crystals, whereas CaO concentrations increase. This is consistent with the diffusion of Fe^{2+} and Mn^{2+} into the olivine from an external source and diffusive loss of Ca^{2+} that would be necessary to convert type 3.0 to type 4 material. The detection limits (D.L.) for individual analyses of MnO and CaO are marked.

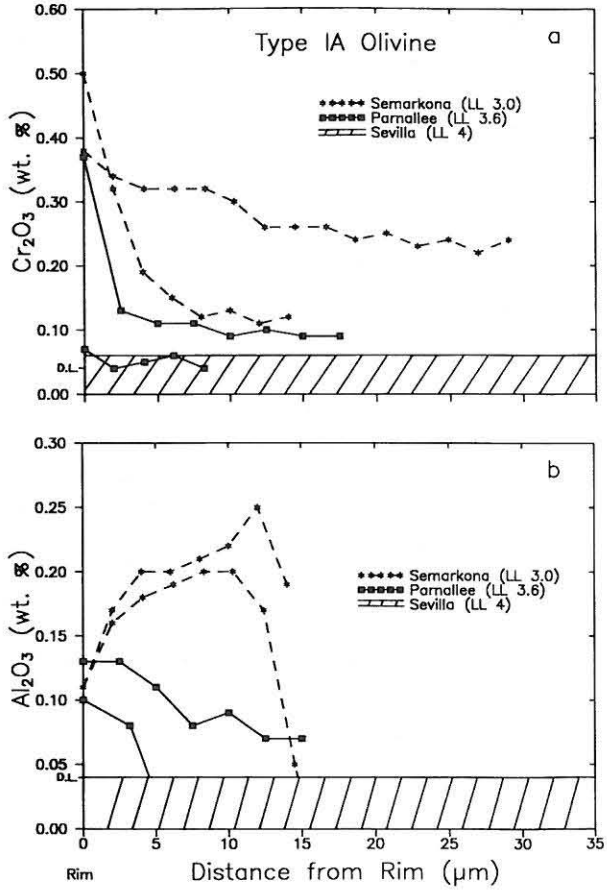

FIG. 4. Rim-to-core zoning profiles for olivine crystals in Semarkona and Parnallee type IA chondrules and the total compositional range observed in Sevilla (LL4): (a) Cr_2O_3 and (b) Al_2O_3. The profiles for Parnallee are atypical in that most olivines have Al_2O_3 concentrations that are below the detection limits (D.L.) and relatively flat Cr_2O_3 profiles. The enrichments of Al_2O_3 and Cr_2O_3 at the rim of Parnallee olivines appear to contradict the trend towards decreasing concentrations in type 4 chondrites and the hypothesis that type 4 chondrites are derived from type 3.0 material. However, the enrichments may be inherited from the precursor type 3.0 material as some Semarkona chondrules also display similar, though more marked, features.

irregular zoning were observed. Similar heterogeneities were first observed by TSUCHIYAMA et al. (1988) in type 3.7–3.9 chondrites. The Fe-rich and Fe-poor bands are parallel to the optical twins.

Changes in the textures of mesostases in type IA chondrules are consistent with increasing recrystallization through the petrologic sequence. For example, in Semarkona (LL3.0), mesostases vary from 100% glass to partly microcrystalline (JONES and SCOTT, 1989), whereas, in Parnallee (LL3.6), they are largely microcrystalline with only small amounts of glass. This glass is mostly found adjacent to pyroxenes, with mesostasis next to olivines being mostly microcrystalline. Mesostasis is almost entirely microcrystalline in chondrules of petrologic type 4 and above. The only exception we observed is a pink, clear, perfectly isotropic glass in a chondrule in Krahenberg (LL5). Its unusual CaO-poor composition (0.14 wt% CaO) may be responsible for its survival in a chondrite

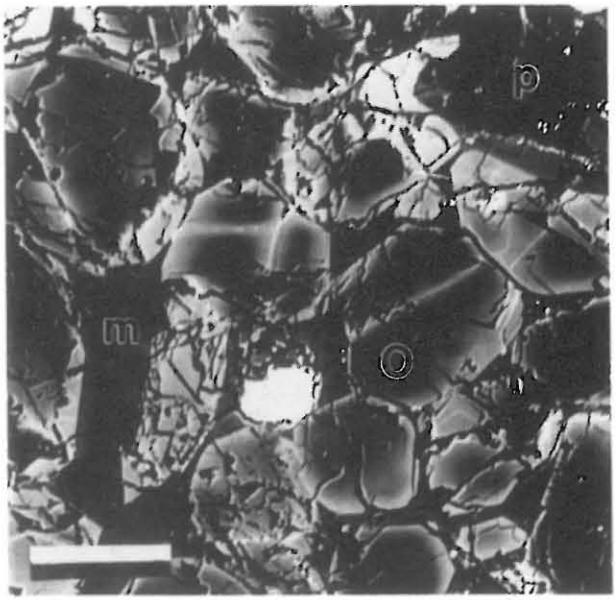

FIG. 5. Back-scattered electron image of a portion of a type IA chondrule in Parnallee, largely composed of olivine phenocrysts (o) with small amounts of mesostasis (m) and low-Ca pyroxene (p). Olivines are mostly whiter at their rims because of FeO enrichments. Some olivines show linear or curvilinear features with associated FeO enrichments (up to Fa_{25}) and bright phases (high in Cr, Al) nucleated within these features. These linear features are interpreted as pre-existing cracks which served as high-diffusivity paths during metamorphism, indicating that FeO enrichment occurred after solidification. Metal occurs to the left of (o) and Fe-enriched olivines to the right of (m) and left of (p). These probably result from sectioning through an Fe-rich rim. Scale bar = 50 μm.

of high petrologic grade. The similarity in olivine phenocryst composition in this chondrule ($Fa_{27.6}$) and other chondrules with CaO-rich mesostases ($Fa_{28.5}$) argues against this chondrule being xenolithic. One chondrule with a glass mesostasis of similar composition (0.89 wt% CaO) was also found in Parnallee (LL3.6) (Table 4). Its mean olivine composition ($Fa_{14.8}$) is close to the mean of olivines in other chondrules ($Fa_{16.8\pm2.0}$).

Mesostasis compositions in type IA chondrules are highly variable even within a given chondrite (Table 4), but trends through the petrologic sequence are observed for FeO, which tends to increase, and TiO_2, which tends to decrease, with increasing petrologic type (Table 4). No systematic differences were observed in bulk compositions of glassy (excluding low-CaO glass) and microcrystalline mesostases in either Semarkona or Parnallee. Two chondrules in Sevilla have mesostases with remarkably high Cr_2O_3 contents of 1.8–2.5 wt% (Table 4). No spinel phases were observed optically in these chondrules, so the host phase for the Cr_2O_3 remains unknown.

Bulk chondrule compositions are also highly variable within a given chondrite (Table 5). Some compositional trends observed for individual components are reflected in the bulk compositional data. Thus, FeO and MnO increase with increasing petrologic type (Table 5).

Type II Chondrules

Except for changes in the grain size of their mesostases, textures of type II chondrules are strikingly similar in LL3.0–5 chondrites (Fig. 10), in spite of drastically different compositions of their olivines.

The mean fayalite concentration of type II chondrules increases and CaO in olivine decreases through the type 3–5 sequence as the degree of heterogeneity within the chondrule decreases (Fig. 11). In LL4–6 chondrites, the fayalite and CaO concentration ranges in type II chondrules are identical to those observed in type IA chondrules. Comparison of chemical data for olivine in type IA (Table 2) and type II chondrules (Table 6) shows that olivine compositions converge to the same composition with increasing degrees of metamorphism. The small differences in the mean Cr_2O_3 and TiO_2 concentrations given in Tables 2 and 6 are not significant as they result from analysis of a small number of grains. In both cases, FeO and MnO increase and CaO and Cr_2O_3 decrease with increasing petrologic type. Al_2O_3 and TiO_2 concentrations decrease in type IA olivines, but the concentrations of these elements are too low in Semarkona type II chondrule olivines to determine if analogous trends exist in type II chondrules.

Table 3. Mean compositions (wt. %) of low-Ca pyroxenes in type IA chondrules from LL3.0-5 chondrites.

Meteorite	Type	SiO_2	TiO_2	Al_2O_3	Cr_2O_3	FeO	MnO	MgO	CaO	Na_2O	Total	Fs	Wo	N*
Semarkona	3.0	57.9	0.20	1.1	0.86	1.2	0.20	36.8	0.94	<0.04	99.24	1.7	1.8	10
		1.1	*0.12*	*0.5*	*0.64*	*0.5*	*0.14*	*1.2*	*0.79*			*0.8*	*1.5*	
ALH A81251	3.3	58.6	0.19	0.94	0.62	1.2	0.12	37.3	0.46	<0.04	99.45	1.7	0.8	4
		0.5	*0.08*	*0.47*	*0.08*	*0.3*	*0.04*	*0.4*	*0.12*			*0.4*	*0.2*	
Parnallee	3.6	58.1	0.13	0.86	0.43	4.1	0.16	35.4	0.56	<0.04	99.78	6.0	1.0	5
		1.2	*0.08*	*0.56*	*0.05*	*2.5*	*0.13*	*2.2*	*0.36*			*3.9*	*0.7*	
Bo Xian	4	57.2	0.13	1.1	0.46	7.9	0.19	32.3	0.55	0.09	100.92	11.6	1.3	5
		1.3	*0.03*	*0.4*	*0.12*	*1.8*	*0.04*	*1.4*	*0.37*	*0.06*		*2.8*	*0.6*	
Sevilla	4	55.6	0.20	0.20	0.14	15.6	0.45	27.6	0.68	<0.04	100.49	23.4	1.3	3
		0.2	*0.05*	*0.02*	*0.02*	*0.1*	*0.01*	*0.3*	*0.10*			*0.2*	*0.2*	
Olivenza	5	55.1	0.23	0.20	0.17	16.3	0.44	27.2	0.78	<0.04	100.44	24.5	1.5	4
		0.9	*0.10*	*0.10*	*0.09*	*0.1*	*0.01*	*0.3*	*0.07*			*0.2*	*0.1*	

* Number of chondrules analyzed.
Italicized figures are standard deviations of the mean compositions of individual chondrules.
Sources: Semarkona, JONES and SCOTT (1989); higher petrologic types, this work.

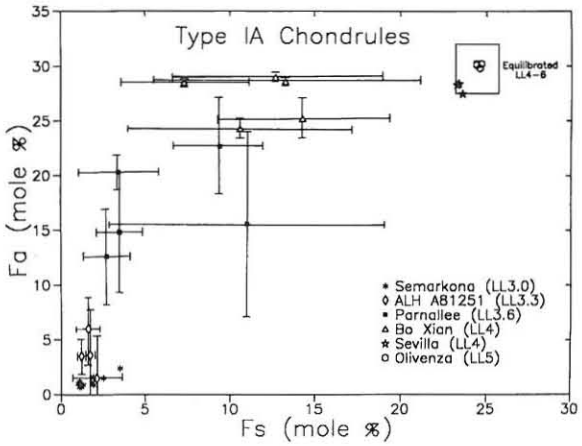

FIG. 6. Mean concentrations of fayalite in olivine and ferrosilite in low-Ca pyroxene in 30 type IA chondrules from 6 LL chondrites; bars show one standard deviation for the analyses in each chondrule. The mean chondrule compositions define a curved path from type 3.0 to type 5–6. This path and the different relative homogeneities of olivine and low-Ca pyroxene in ALH A81251 (type 3.3) and Bo Xian (type 4) are both consistent with the conversion of Semarkona-like chondrules to type 4–6 chondrules by equilibration with FeO-enriched silicates in the matrix and other chondrules, as Fe-Mg diffusion is faster in olivine than in pyroxene. The Semarkona data are from JONES and SCOTT (1989), and the compositional ranges for equilibrated LL4–6 chondrites are from GOMES and KEIL (1980).

Zoning profiles of CaO and FeO concentrations in olivine from type II chondrules in Parnallee (LL3.6) are intermediate in nature between those in LL3.0 and LL4 chondrites (Fig. 12a,b). FeO and CaO concentrations are both enriched in the rims of olivine crystals in Semarkona (Fig. 12b; JONES, 1990). In Parnallee, FeO is enriched at olivine rims, whereas

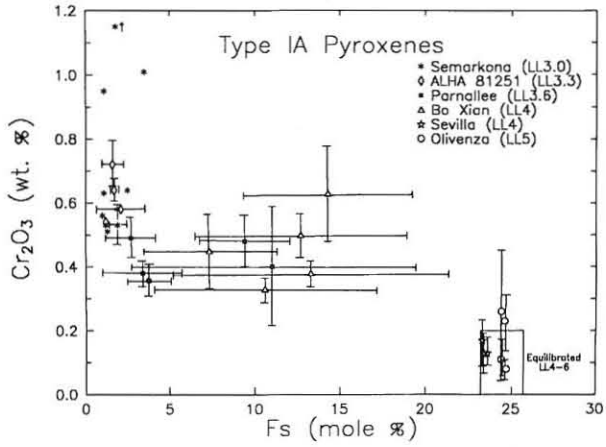

FIG. 7. Mean concentrations of Cr_2O_3 and ferrosilite in low-Ca pyroxenes from 31 type IA chondrules in 6 LL3.0–5 chondrites. In Semarkona (LL3.0), between-chondrule variability is high, but within-chondrule variability is low; both are high in intermediate types, and lowest in equilibrated LL4–6 chondrites. Bars indicate one standard deviation for 5 to 15 analyses in each chondrule. Semarkona data are from JONES and SCOTT (1989). The equilibrated LL4–6 rectangle represents the range of chondrite average values from low-Ca pyroxenes in equilibrated LL chondrites. Data for Cr_2O_3 are from GOMES and KEIL (1980) and this work; data for Fs are from GOMES and KEIL (1980).

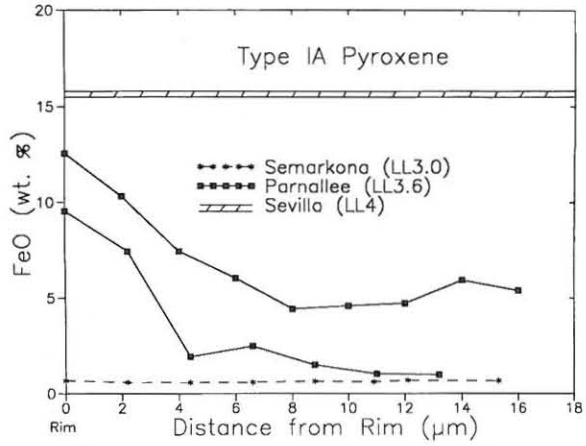

FIG. 8. Zoning profiles for FeO measured from rim to core across two typical low-Ca pyroxene grains in type IA chondrules in Parnallee (LL3.6), one in Semarkona (LL3.0), and the total range of FeO in three type IA chondrules in Sevilla (LL4). Low-Ca pyroxene grains in the type 3.0 chondrite have essentially no zoning; in the LL3.6 chondrite they have elevated FeO concentrations and are strongly zoned with FeO increasing towards the rim; and in Sevilla (and more equilibrated type 4–6 chondrites), FeO concentrations are high and uniform.

CaO is depleted, consistent with loss of CaO but gain of FeO. As in type IA chondrules, olivine phenocrysts in type II chondrules in chondrites of petrologic type 3.3 and 3.6 have

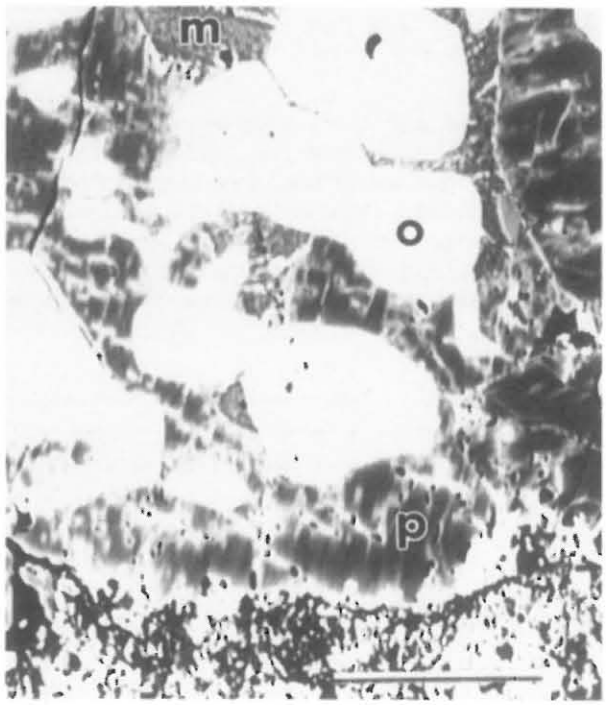

FIG. 9. Back-scattered electron SEM image of low-Ca pyroxene (p), olivine (o), and mesostasis (m) in a type IA chondrule of Bo Xian (LL4). Unlike low-Ca pyroxene grains in Parnallee which are smoothly zoned (Fig. 3), those in Bo Xian have very heterogeneous Fe-Mg contents, indicated by irregular white (FeO) enrichments and light/dark bands near (p). TSUCHIYAMA et al. (1988) observed similar phenomena in H, L, and LL chondrites of petrologic type 3.7–3.9. Scale bar equals 50 μm.

Table 4. Composition (wt. %) of mesostasis in type IA chondrules from LL3.0-5 chondrites.

Meteorite	Type	Chondrule	SiO_2	TiO_2	Al_2O_3	Cr_2O_3	FeO	MnO	MgO	CaO	Na_2O	K_2O	P_2O_5	Total	N*
Semarkona	3.0		52.5	0.85	21.8	0.42	0.74	0.12	5.1	15.6	1.8	0.18	n.d.	99.11	8
			7.4	*0.33*	*4.8*	*0.30*	*0.44*	*0.10*	*1.3*	*4.6*	*2.0*	*0.24*			
Parnallee	3.6	5	57.9	0.47	20.2	0.59	3.6	0.07	4.2	0.89	8.9	3.4	<0.05	100.24	7
		6	52.2	0.52	21.9	0.46	3.7	0.15	4.3	10.1	4.9	0.19	0.13	98.55	7
		7	55.3	0.46	21.1	0.33	3.4	0.06	4.5	8.9	5.8	0.25	0.11	100.21	6
		9	61.7	0.42	16.0	0.46	2.4	0.14	4.3	3.9	8.0	1.1	0.11	98.53	6
		10	50.9	0.71	18.9	0.48	3.8	0.19	10.4	12.1	2.7	0.14	0.14	100.46	5
		14	52.3	0.48	20.6	0.17	3.6	0.07	5.4	11.2	4.0	0.43	0.12	98.37	5
Sevilla	4	1	56.2	0.37	15.7	2.5	7.3	0.20	9.6	3.0	6.0	0.15	<0.05	101.02	2
		5	56.5	0.14	15.3	1.8	7.6	0.17	9.6	2.7	6.3	0.36	<0.05	100.50	5
		A5	60.4	0.08	17.8	1.0	4.7	0.09	5.3	3.0	7.8	0.47	0.05	100.69	3
		A7	59.7	0.14	14.2	0.16	4.7	0.12	7.7	6.3	6.8	0.38	0.14	100.34	5
Olivenza	5	A3	59.3	0.25	13.4	0.53	3.7	0.11	6.3	10.1	6.0	0.53	0.06	100.28	2
Equil. Chon.†		Avg.	58.4	0.20	15.3	1.2	5.6	0.14	7.7	5.0	6.6	0.38	0.07	100.59	
		σ	*1.9*	*0.12*	*1.7*	*0.95*	*1.7*	*0.05*	*1.9*	*3.2*	*0.76*	*0.14*	*0.04*		

* For Semarkona, N = Number of chondrules averaged; for higher petrologic types, N = number of individual analyses.
† Average of chondrules from Sevilla and Olivenza.
Sources: Semarkona, JONES and SCOTT (1989); higher petrologic types, this work.

linear features high in Cr and Al and adjacent areas with elevated iron contents, suggesting that they served as high-diffusivity paths during alteration. Chromium- and aluminum-rich cracks are also present in type 4–6 chondrites.

Textures of mesostases in type II chondrules are consistent with increasing degree of recrystallization from lower to higher petrologic type chondrites. For example, textures of mesostases vary from glassy with abundant microcrystallites in Semarkona to completely microcrystalline in equilibrated chondrites. Quench crystals are common in mesostases throughout the petrologic sequence. In Parnallee these crystals are augite in a largely microcrystalline mesostasis which has only rare, small areas of glass. Mesostasis bulk compositions are highly variable but show decreasing FeO and MnO with increasing petrologic type (Table 7).

Bulk compositions reflect compositional changes of individual components in type II chondrules. It appears that bulk FeO and CaO increase and Cr_2O_3 decreases with increasing petrologic type (Table 8).

DISCUSSION

The data presented above can be used to evaluate the various proposed origins for the formation of the petrologic sequence. This is done below by evaluating both textural and chemical data and modelling of diffusive equilibration of chondrule silicates. We first consider models which ascribe the formation of the petrologic sequence to differences during chondrule crystallization. We then consider two processes that call for diffusive equilibration of solidified chondrules: nebular metasomatism and parent body metamorphism.

Table 5. Bulk compositions (wt. %) of type IA chondrules in LL3.0-5 chondrites.

Meteorite	Chondrule	SiO_2	TiO_2	Al_2O_3	Cr_2O_3	FeO	MnO	MgO	CaO	Na_2O	K_2O	P_2O_5	Silicate Total	FeS	Fe,Ni
Semarkona*		44.8	0.19	3.9	0.44	1.2	0.12	40.7	3.5	0.52	0.07	n.d.		0.20	3.8
		3.2	*0.08*	*1.2*	*0.30*	*0.9*	*0.08*	*3.6*	*1.3*	*0.59*	*0.06*			*0.13*	*2.0*
Parnallee	5	47.0	0.10	3.0	0.39	10.7	0.21	36.3	0.54	1.4	0.55	<0.04	100.20	5.5	4.6
	6	45.9	0.23	5.0	0.46	8.3	0.20	34.9	2.9	1.1	0.07	0.12	99.18	1.2	1.3
	7	41.9	0.13	2.9	0.32	16.4	0.23	35.6	1.6	0.75	0.07	<0.04	99.93	8.3	9.7
	9	48.9	0.15	3.4	0.62	10.6	0.32	29.9	2.1	1.9	0.25	<0.04	98.17	0.27	0.66
	10	39.9	0.17	3.9	0.32	13.4	0.20	37.2	2.2	0.70	0.06	0.09	98.14	1.6	1.8
	14	43.7	0.20	6.1	0.18	13.0	0.23	30.5	3.7	0.99	0.14	0.04	98.78	14.5	10.6
Sevilla	5	42.8	0.09	2.5	0.40	21.3	0.43	30.5	0.85	1.1	0.11	0.08	100.16	0.96	4.9
	6	42.6	<0.09	2.5	0.40	21.5	0.42	30.9	0.51	1.4	0.09	<0.04	100.38	4.4	6.4
	A4	46.1	<0.09	4.1	0.21	16.9	0.33	25.4	4.2	2.2	0.17	0.62	100.31	8.5	0.44
	A7	46.5	0.09	2.9	0.21	18.0	0.36	27.3	3.4	1.5	0.13	0.04	100.43	1.9	1.3
Olivenza	3	43.7	0.10	3.1	0.52	21.0	0.41	28.9	0.43	1.3	0.15	<0.04	99.62	0.41	0.22
	5	49.4	0.13	2.9	0.16	18.2	0.40	27.2	1.2	1.5	0.15	<0.04	101.25	3.7	2.0
	A3	47.4	0.16	3.7	1.1	19.9	0.42	27.1	0.74	1.6	0.18	<0.04	102.31	2.0	0.44
Equil. Chon.†	Avg.	45.5	0.10	3.1	0.43	19.5	0.40	28.2	1.6	1.5	0.14	0.11	100.58	3.1	2.2
	σ	*2.6*	*0.04*	*0.60*	*0.32*	*1.8*	*0.04*	*2.0*	*1.5*	*0.34*	*0.03*	*0.23*		*2.8*	*2.5*

n.d. - Not Determined.
* Mean and 1σ for 11 chondrules.
† Average of chondrules from Sevilla and Olivenza.
Sources: Semarkona, JONES and SCOTT (1989); higher petrologic types, this work.

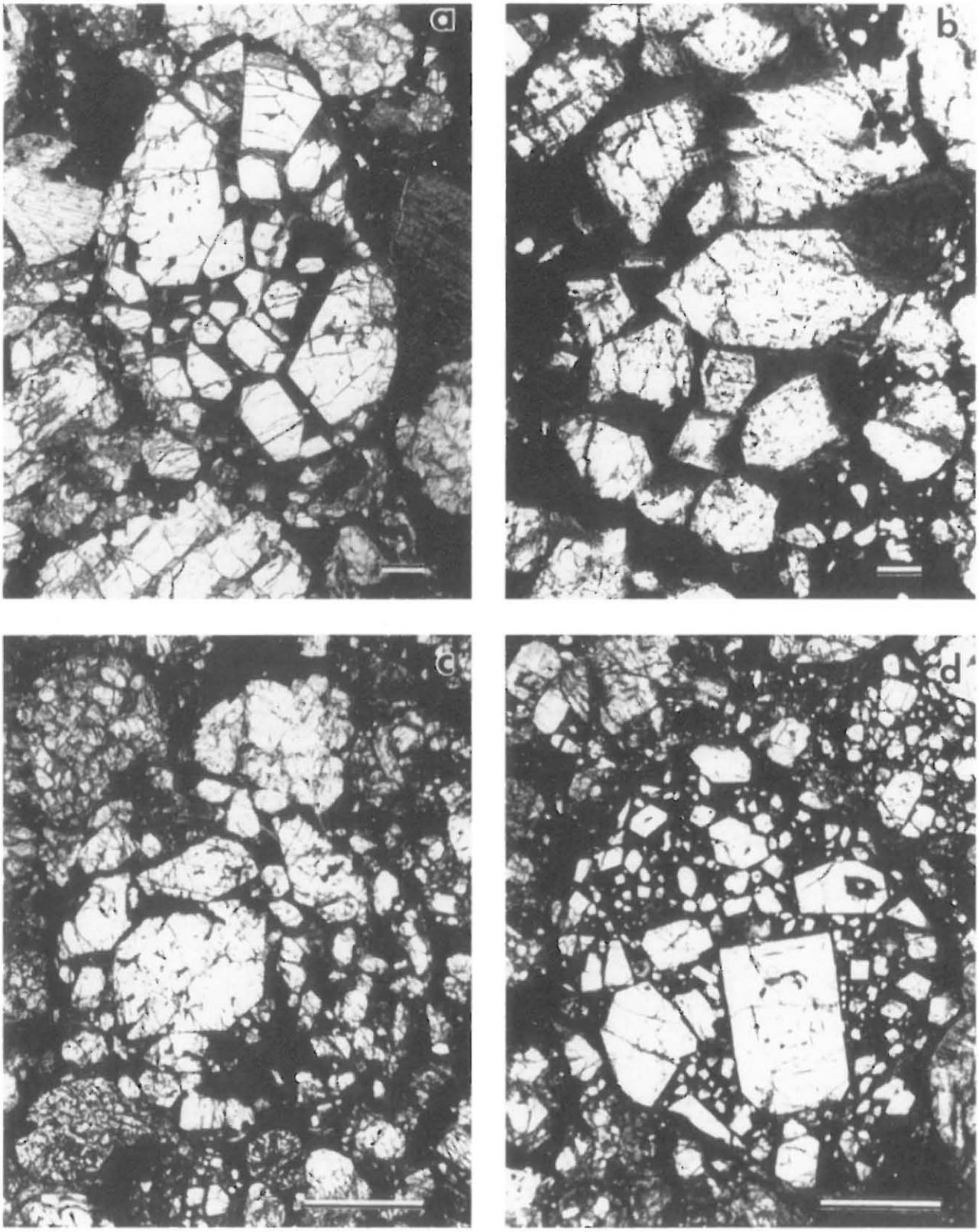

FIG. 10. Transmitted light photomicrographs of type II chondrules, which consist of large euhedral olivines set in dark microcrystalline mesostasis, in LL chondrites: (a) Semarkona, type 3.0; (b) Allan Hills A81251, type 3.3; (c) Parnallee, type 3.6; and (d) Bo Xian, type 4. Petrographic properties of these chondrules are very similar, suggesting that they crystallized under similar conditions. Their diverse olivine compositions reflect igneous zoning (a) and subsequent equilibration (b–d). Mean olivine compositions and standard deviations of the 5 to 37 analyses in each chondrule are as follows: (a) Fa12 ± 4, (b) Fa15 ± 6, (c) Fa24 ± 4, (d) Fa29 ± 0.2. Scale bar = 200 μm.

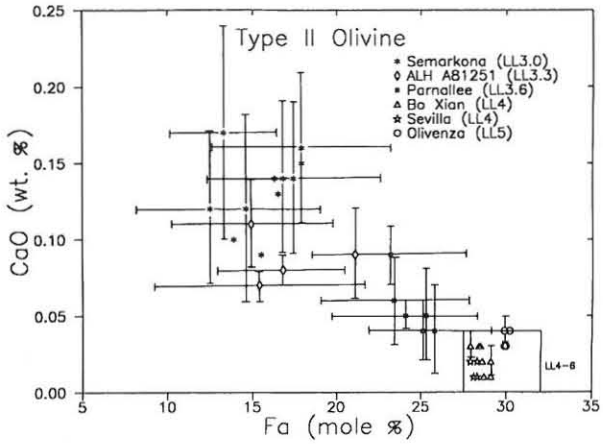

FIG. 11. Mean concentrations of CaO and fayalite in olivine crystals from 36 type II chondrules in 6 LL3.0–5 chondrites. Bars indicate one standard deviation for individual analyses in each chondrule; bars are omitted from five chondrules in Semarkona and all chondrules from equilibrated type 4–5 chondrites to avoid confusion. Mean FeO concentrations increase, CaO concentrations decrease, and chondrule olivines become more homogeneous with increasing chondrite petrologic type. The similarity of olivine compositions in type IA and II chondrules in type 4–5 chondrites suggests that olivines equilibrated during metamorphism.

Crystallization Models

Several authors (REID and FREDRIKSSON, 1967; FREDRIKSSON, 1983; KRING, 1985) and an anonymous reviewer of this paper have argued that compositional changes in chondrules of type 3–4 chondrites reflect differences in the histories of these chondrules during crystallization. HEWINS (1989) reviewed these models and emphasized the importance of nebular processes. He has since, however, changed his conclusions (R. HEWINS, pers. comm., 1990). REID and FREDRIKSSON (1967) argue that the compositional differences between chondrule silicates in all petrologic types of ordinary chondrites result from different rates of crystallization of the molten droplets. KRING (1985) argues that changes in oxygen fugacity during chondrule crystallization resulted in compositional differences between olivines and pyroxenes. JOHNSON (1986) suggests that oxidation of Fe,Ni metal during chondrule crystallization produced the differences in FeO content of chondrule silicates. However, since no systematic trend is observed in the Fe,Ni or troilite contents of type IA or type II chondrules throughout the petrologic sequence, this model is not likely to be applicable and is not discussed further. In all these models, textural differences within type 4–6 chondrites result from parent body metamorphism.

Models that attribute differences in silicate compositions solely to crystallization require a separate formation zone in the solar nebula for each chemical group and petrologic type. In each of the zones, all the chondrule precursors would have to have similar Fe/(Fe + Mg) ratios and cool at similar rates. Furthermore, no mixing between regions could occur during subsequent parent body accretion.

Two lines of evidence suggest that differences between the compositions of chondrule silicates in type 3 and type 4–6 chondrites are not the result of differences in chondrule crystallization histories.

Zoning adjacent to cracks

One line of evidence is the observation that olivine compositions have been changed near linear features that we interpret to be pre-existing cracks (Fig. 5). Although we cannot determine when the cracks formed, they must have formed after solidification of the olivines. Cracks in chondrule olivines show a variety of features which indicate a protracted history of secondary modification. In type IA and II chondrules in type 3.3–4 chondrites, there are commonly FeO enrichments on either side of these crack-like features, accompanied by unidentified Cr- and Al-rich phases that appear to have nucleated in the cracks. This suggests that these cracks acted as high-diffusivity paths during metamorphism, allowing Fe^{2+} to enter along the cracks and Cr^{3+} and Al^{3+} to diffuse out of the olivine structure into the cracks. Some cracks do not show these secondary features, and we believe these cracks formed after the metamorphism.

Table 6. Mean composition (wt. %) of olivines in type II chondrules in LL3.0-5 chondrites.

Meteorite	Type	SiO_2	TiO_2	Al_2O_3	Cr_2O_3	FeO	MnO	MgO	CaO	Total	Fa	N*
Semarkona	3.0	39.4	<0.02	<0.04	0.43	14.8	0.34	44.4	0.13	99.58	15.7	11
		0.3			*0.05*	*1.6*	*0.04*	*1.3*	*0.02*		*1.9*	
ALH A81251	3.3	39.3	0.02	<0.04	0.16	16.1	0.44	44.1	0.09	100.24	17.1	4
		0.5	*0.01*		*0.05*	*2.5*	*0.05*	*2.1*	*0.02*		*2.8*	
Parnallee	3.6	37.9	<0.02	<0.04	0.03	22.8	0.44	39.2	0.06	100.47	24.5	6
		0.1			*0.01*	*0.9*	*0.03*	*0.9*	*0.02*		*1.1*	
Bo Xian	4	37.4	<0.02	<0.04	0.02	26.0	0.45	36.9	<0.04	100.81	28.6	7
		0.3			*0.01*	*0.4*	*0.01*	*0.3*			*0.4*	
Sevilla	4	38.0	<0.02	<0.04	<0.02	25.9	0.45	36.9	<0.04	101.30	28.2	4
		0.4				*0.1*	*0.01*	*0.5*			*0.2*	
Olivenza	5	37.8	<0.02	<0.04	0.02	27.4	0.44	35.6	0.04	101.31	30.0	4
		0.2			*0.01*	*0.2*	*0.01*	*0.1*	*0.01*		*0.1*	

* Number of chondrules analyzed.
Italicized figures are standard deviation of the mean compositions of individual chondrules.
Sources: Semarkona, JONES (1990); higher petrologic types, this work.

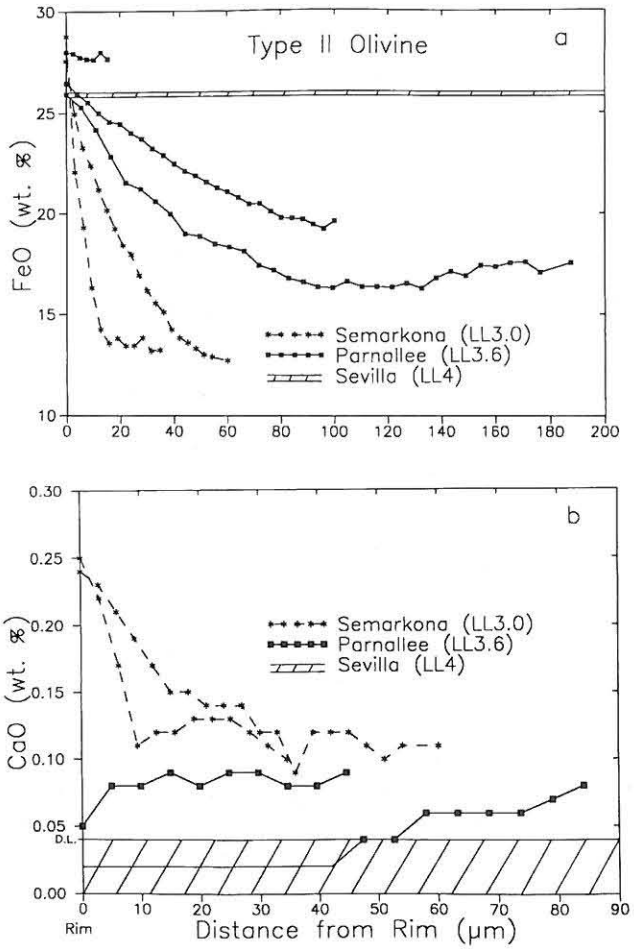

FIG. 12. Zoning profiles for (a) FeO and (b) CaO measured from rim to core of typical olivine crystals in type II chondrules in Semarkona (JONES, 1990) and Parnallee, and the total ranges in type II chondrules in Sevilla (LL4). FeO concentrations in type 3.0 and 3.6 chondrites are enriched at olivine rims, but core concentrations in type 3.6 are higher than those in type 3.0, consistent with diffusion of Fe^{2+} into chondrule olivines during metamorphism. CaO concentrations are enriched in olivine rims in the LL3.0 chondrite, whereas in the LL3.6 chondrite, CaO is depleted in olivine rims and generally lower at the olivine core; both are features consistent with diffusive loss of Ca^{2+} during metamorphism.

Chondrule textures

Throughout the petrologic sequence of type 3–5 chondrites, type IA (Fig. 1) and type II (Fig. 10) chondrules remain texturally unchanged, with the exception of mesostasis devitrification and coarsening. As shown by DONALDSON (1976), the morphology of olivine crystals is a strong function of cooling rate. This implies a common crystallization history for all type IA chondrules. Likewise, all type II chondrules must have had a similar crystallization history. It is unlikely that the markedly different crystallization histories that REID and FREDRIKSSON (1967) invoke to explain compositional differences could result in the textural similarities observed throughout the petrologic sequence. Although we do not know the exact sensitivity of the porphyritic olivine texture to cooling rate, the vast range of cooling rates proposed by REID and FREDRIKSSON (1967) to produce chondrules in type 3–6 chondrites would likely produce a variety of textures.

Planetary Metamorphism and Nebular Metasomatism

Two processes have been proposed to explain chemical modification of chondrule silicates after solidification of the chondrules: nebular metasomatism and parent body metamorphism. KURAT (1988) suggests that chondrules were altered by interaction with a nebular gas, whereas DODD (1969) argues that the chemical changes result from metamorphic equilibration with other chondritic components in the parent body. To a certain extent, a gradation exists between these two models because chondrules would aggregate into intermediate sized objects before forming the parent body. Metamorphism inside boulder-sized objects would be essentially the same as in a parent body, except that chondritic components might continue to react with the nebula as well.

Chemical trends and complexities

Elemental concentrations in olivines, pyroxenes, and mesostases of type IA and type II chondrules and their bulk compositions show systematic progression from values like those in Semarkona, through the LL3.3, 3.6, and 4 chondrites to the values of the equilibrated LL chondrites. Concentrations of FeO increase in olivines, pyroxenes, mesostasis, and bulk chondrules of both type IA and type II chondrules, with corresponding decreases in MgO. MnO increases in type IA olivines, pyroxenes, and bulk chondrules and type II olivines and bulk chondrules. CaO decreases in type IA and II olivines and increases in type II bulk chondrules. Al_2O_3 and Cr_2O_3 decrease in type IA olivines and pyroxenes. TiO_2 decreases in type IA olivines and mesostasis. Additionally, mesostasis devitrification increases progressively from type 3.0 to type 4–5.

Subsolidus equilibration of chondrule silicates requires the homogenization of initially zoned mineral grains, equilibration of minerals within each chondrule, and equilibration of diverse minerals in chondrules and matrix material. This subsolidus equilibration may also have involved phases in a nebular gas, and new phases may have nucleated during the modification. Therefore, one ought not to expect that every chemical trend for minerals in type 3.0–5 chondrites be simple and monotonic. The fact that we have identified so many monotonic trends in the type 3.0–5 chondrites suggests that type 3.1–3.9 chondrites did not originate in any fundamentally different way from type 4–6 chondrites, and that type 3.0 material is the best candidate for the precursor material of type 3.3–5 material. We see no evidence favoring the conclusion of GUIMON et al. (1988) that type 3.3 ordinary chondrites represent the precursor materials for type 3.0–3.2, as well as type 3.4–6.

Environment of diffusive exchange

Several authors have called upon mechanisms involving condensation and diffusive exchange with a nebular gas at high temperatures and oxygen fugacities to explain Fe-enrichment in chondrule olivines of CV3 chondrites (PECK and WOOD, 1987; PALME and FEGLEY, 1987, 1991). HUA et al.

Table 7. Composition (wt. %) of mesostases in type II chondrules from LL3.0-5 chondrites.

Meteorite	Type	Chondrule	SiO_2	TiO_2	Al_2O_3	Cr_2O_3	FeO	MnO	MgO	CaO	Na_2O	K_2O	P_2O_5	Total	N*
Semarkona	3.0		62.6	0.45	11.2	0.30	7.8	0.28	4.5	7.2	4.1	0.58	1.3	100.31	10
			1.5	*0.04*	*1.5*	*0.14*	*1.2*	*0.07*	*1.7*	*1.7*	*1.5*	*0.13*	*1.0*		
Parnallee	3.6	1	68.6	0.41	10.0	0.36	6.8	0.25	2.9	4.6	5.8	0.70	0.39	100.81	9
		2	62.0	0.46	10.3	0.27	6.5	0.25	4.4	9.5	6.0	0.10	0.93	100.71	9
		4	59.2	0.48	10.1	0.28	7.2	0.23	5.0	10.4	6.4	0.09	1.6	100.98	9
		11	66.5	0.44	9.3	0.47	6.0	0.27	4.7	6.6	5.8	0.15	0.32	100.55	9
		12	67.8	0.41	10.4	0.40	3.4	0.18	4.5	6.1	5.8	0.69	0.19	99.87	9
		13	60.4	0.46	9.9	0.24	7.1	0.27	5.1	9.7	5.9	0.41	1.3	100.78	9
Sevilla	4	2	57.5	0.15	12.4	0.24	3.3	0.10	6.9	10.7	6.2	0.37	1.5	99.36	4
		4	57.6	0.17	12.7	0.24	4.1	0.10	7.8	10.0	6.1	0.38	1.3	100.49	5
		A1	60.4	0.19	12.8	0.28	2.7	0.10	6.4	10.9	6.0	0.41	0.50	100.68	2
		A2	58.3	0.29	9.7	0.50	3.6	0.14	9.2	14.1	4.5	0.34	0.38	101.05	6
		A3	58.1	0.32	8.4	0.50	3.6	0.15	10.1	15.0	4.1	0.26	0.26	100.79	8
		A4	56.7	0.19	11.7	0.27	4.9	0.12	8.6	10.8	5.6	0.38	1.2	100.46	3
Olivenza	5	A1	56.9	0.27	7.8	0.43	3.9	0.16	10.2	16.1	3.6	0.34	0.52	100.22	5
Equil. Chon.†		Avg.	57.9	0.23	10.8	0.35	3.7	0.12	8.5	12.5	5.2	0.35	0.81	100.46	
		σ	*1.2*	*0.07*	*2.1*	*0.12*	*0.68*	*0.03*	*1.5*	*2.5*	*1.1*	*0.05*	*0.51*		

* For Semarkona, N = number of chondrules analyzed; for higher petrologic types, N = number of individual analyses.
† Average of chondrules from Sevilla and Olivenza.
Sources: Semarkona, JONES (1990); Higher petrologic types, this work.

(1988) found that sharp compositional gradients exist in olivines near chondrule rims and reasoned that these are produced by condensation of a Fa-rich rim onto a forsteritic core. These gradients are quite different from the smooth FeO profiles found in LL3.3 and 3.6 chondrule olivines. These smooth profiles in LL3 chondrites are similar to those reproduced in diffusion calculations for CO3 chondrites (JONES and RUBIE, 1990) for the case of parent body metamorphism. The formation of FeO-bearing olivine at high temperatures requires a gas phase that is significantly more oxidizing than a solar composition gas (PALME and FEGLEY, 1991). Under these conditions, MnO contents of olivines are also expected to increase with FeO contents (PALME and FEGLEY, 1991). This trend is observed in chondrule olivines. Thus, compositional constraints obtained from chondrules are consistent with the limited predictions available for a nebular metasomatism model.

Diffusive exchange *in situ* between the various components of an accreted chondrite is considerably more complex. Minerals in type IA and II chondrules can exchange with minerals in several other common types of chondrules, as well as isolated mineral fragments and fine-grained matrix minerals.

Table 8. Bulk compositions (wt. %) of type II chondrules in LL3.0-5 chondrites.

Meteorite	Chondrule	SiO_2	TiO_2	Al_2O_3	Cr_2O_3	FeO	MnO	MgO	CaO	Na_2O	K_2O	P_2O_5	Silicate Total	FeS	Fe,Ni
Semarkona*		45.1	0.10	2.7	0.51	14.9	0.39	31.3	1.9	1.7	0.17	0.34		0.94	0.51
		2.0	*0.02*	*0.54*	*0.06*	*1.7*	*0.05*	*2.7*	*0.30*	*0.35*	*0.07*	*0.29*		*1.2*	*0.57*
Parnallee	1	46.3	0.09	1.8	0.35	14.7	0.42	33.7	1.7	1.0	0.16	0.08	100.30	0.41	0.66
	2	43.8	0.11	2.1	0.53	19.3	0.38	31.6	2.0	1.4	0.08	0.19	101.80	0.41	0.22
	4	42.4	0.11	2.4	0.4	19.5	0.37	31.2	1.7	1.4	0.08	0.35	99.91	0.68	0.66
	11	47.3	0.13	2.5	0.33	14.1	0.39	32.1	1.6	1.5	0.16	0.09	100.20	0.55	0.44
	12	43.5	<0.09	1.7	0.41	15.0	0.38	35.7	1.3	0.78	0.36	0.06	99.25	0.14	0.22
	13	47.0	0.17	4.0	0.64	15.1	0.34	24.7	3.4	2.5	0.14	0.46	98.41	0.41	0.00
Sevilla	A1	47.1	0.11	2.0	0.21	17.8	0.40	28.7	3.2	1.2	0.11	0.07	100.90	0.27	0.00
	A2	44.1	<0.09	2.4	0.18	19.4	0.44	29.6	3.3	1.3	0.13	0.06	100.98	1.9	0.44
	A3	43.3	0.10	2.1	0.33	19.3	0.39	29.5	3.6	1.2	0.17	<0.04	100.02	0.27	0.44
	A5	45.8	0.10	2.9	0.22	17.5	0.38	27.3	4.3	1.5	0.14	<0.04	100.16	0.14	0.00
Olivenza	1	45.3	<0.09	3.9	0.15	18.0	0.36	25.0	4.1	2.1	0.22	0.14	99.35	0.27	0.00
	4	44.4	<0.09	3.6	0.25	19.3	0.37	26.7	2.9	1.9	0.17	0.13	99.78	1.9	0.00
	A1	44.4	0.10	1.7	0.20	20.0	0.43	28.6	4.4	0.91	0.11	0.15	101.00	0.27	0.00
	A2	43.6	<0.09	3.9	0.09	20.5	0.37	27.5	2.4	2.0	0.22	0.18	100.80	1.5	3.1
Equil. Chon.†	Avg.	44.8	0.08	2.8	0.20	19.0	0.39	27.9	3.5	1.5	0.16	0.10	100.43	0.82	0.50
	σ	*1.3*	*0.02*	*0.89*	*0.07*	*1.1*	*0.03*	*1.6*	*0.71*	*0.44*	*0.04*	*0.06*		*0.80*	*1.1*

n.d. - Not Determined.
* Mean and 1σ of 11 chondrules.
† Average of chondrules from Sevilla and Olivenza.
Sources: Semarkona, JONES (1990); higher petrologic types, this work.

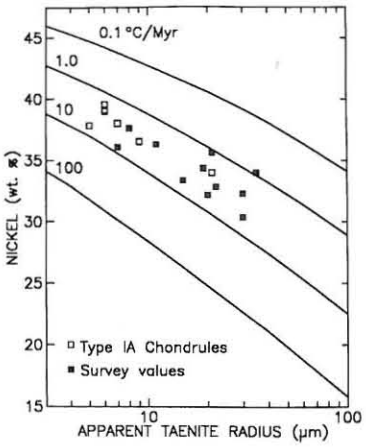

FIG. 13. Metallographic cooling rate data for Parnallee (LL3.6). A coherent cooling rate of 10°C/Ma is indicated by taenite grains from both within type IA chondrules (open squares) and throughout the meteorite (filled squares). The lowest nickel content in a taenite core indicates a peak metamorphic temperature of at least 520°C. Cooling to 300°C would require about 22 million years, much longer than the lifetime of the solar nebula. Cooling rate curves are from WILLIS and GOLDSTEIN (1981a).

HUSS et al. (1981) analyzed fine-grained matrix in type 3 ordinary chondrites and observed correlations indicating compositional exchange between chondrule and matrix olivines with increasing petrologic subtype. They inferred that Semarkona matrix was the least metamorphosed and that fine-grained matrix in LL chondrites shows decreasing FeO and increasing MgO with increasing petrologic subtype and little change in CaO and Al_2O_3, which is consistent with observed trends in chondrule compositions. HUSS et al. (1981) point out that there is also primary chemical variation within matrix of unequilibrated ordinary chondrites. In addition to chondrule-matrix interaction, inter-chondrule equilibration is likely to be an important process during *in situ* metamorphism. MnO trends in type IA and II chondrules with increasing petrologic type could to a large extent be the result of equilibration between the two chondrule types alone. It is clear that compositional constraints are entirely consistent with metamorphism in a parent body.

We now consider the mechanisms of diffusive transfer, in order to examine any constraints which may be imposed in either a nebular or planetary environment. Diffusion pathways within the chondrules studied are clearly observed in the back-scattered electron images of Figs. 1 and 5: iron enrichment occurs along grain boundaries and cracks in olivines and pyroxenes. In the nebula, gas can penetrate into the chondrule along cracks and grain boundaries, but, in the parent body, solid-state diffusion is the only viable mechanism. Grain-boundary diffusion and surface diffusion are considerably faster than lattice diffusion, particularly at low temperatures, so that observed diffusion pathways are also consistent with parent-body metamorphism.

In summary, compositional constraints on the environment of diffusive exchange provide no firm conclusions to favor either a nebular metasomatism or planetary metamorphism model. A consideration of time scales for metamorphism, discussed in detail below, provides less ambiguous evidence which favors planetary metamorphism over nebular metasomatism.

Time Scales for Chondrule Alteration

The times required for chondrule modification can help distinguish between nebula metasomatism and parent body metamorphism. As WOOD and MORFILL (1988) show in their review, the solar nebula lasted no more than one million years. Below, we estimate the time scales for chondrule modification using metallographic cooling rates, Fe-Mg diffusion in olivines and pyroxenes, and minor element diffusion in olivine.

Metallographic cooling rates

WOOD (1967) demonstrated that the relationship between the apparent size of a taenite grain and the Ni content at its center could be used to determine the cooling rate of a chondrite. Metallographic cooling rate data for Parnallee (LL3.6) are presented in Fig. 13. Taenites in type IA chondrules and elsewhere in the meteorite plot coherently and indicate a cooling rate of 10°C/Ma. The coherence of the metallographic cooling rate indicates that all the components were assembled prior to metamorphism. Because of geometric effects, the cooling rate is determined from the lower envelope of the data. We can estimate the minimum peak temperature during metamorphism from the lowest Ni content in taenite centers and plotting this on the Fe-Ni phase diagram. A temperature of at least 520°C is suggested. This temperature is 100°C higher than that suggested for type 3.6 ordinary chondrites by BREARLEY (1990) based on graphitization of carbon-rich material. The difference in temperatures between the two thermometers may not be significant when errors are considered. We prefer to use the metallographic peak temperature which we have measured for Parnallee, rather than the graphite temperatures which were determined for other type 3 chondrites.

Cooling from 520 to 300°C at 10°C/Ma would require about 22 million years, strongly favoring planetary metamorphism, since this time is considerably longer than maximum estimates for nebular collapse. WILLIS and GOLDSTEIN (1981a) estimate that their cooling rate curves may be in error by a factor of 2. However, a time of 11 million years is still needed for cooling to 300°C. WILLIS and GOLDSTEIN (1981a) caution against the use of these curves for meteorites containing high levels of phosphorus. However, the zoned taenites we measured to determine the metallographic cooling rate in Parnallee contain <0.02 wt% phosphorus.

Time scales for chondrule equilibration suggested by Parnallee metallographic cooling rate data agree well with time scales suggested for equilibrated chondrites by a number of other methods. As summarized by WILLIS and GOLDSTEIN (1981a), most ordinary chondrites cooled through 500°C at rates of 1–10°C/Ma. TURNER et al. (1978) found ages of 4.50–4.44 Ga for ordinary chondrites using ^{40}Ar-^{39}Ar age dating techniques. These ages imply that chondrites required tens of millions of years to cool to the closure temperature of the ^{40}Ar-^{39}Ar system. Cooling rates by ^{244}Pu fission-track thermometry (PELLAS and STORZER, 1981) also require tens to hundreds of millions of years for metamorphism of or-

dinary chondrites. Thus, all of these very different methods for determining time scales for metamorphism suggest periods much greater than one million years, consistent with parent body metamorphism.

Iron-magnesium Diffusion in Olivine

Chondrite cooling rates are consistent with parent body metamorphism: the nebula simply cools too fast. However, the cooling rates alone do not prove that the trends we observe in porphyritic olivine chondrules were established solely on the parent body.

Further constraints can be placed on metamorphic time scales by comparing time scales suggested by metallographic cooling rate data with those for equilibration of Fe-Mg profiles by diffusion in chondritic olivines. Our calculations model the homogenization of olivine grains rather than the exchange between olivines and a matrix reservoir, and are thus more simplified than similar calculations performed by MIYAMOTO et al. (1986) and JONES and RUBIE (1990). We assume that volume diffusion through the olivines is the rate determining step. This is a reasonable approximation, in view of the similarity in zoning between olivines in type IA chondrules and isolated olivines in direct contact with matrix (Fig. 1b), as well as a lack of correlation between the percent of glass in the mesostasis and the composition of the chondrule silicates, which demonstrates the ease of diffusion through the fine-grained mesostasis.

Our calculations determine the average Fe diffusion distance in olivine as a function of peak metamorphic temperature and cooling rate. We use the relation $X^2 = 2Dt$, where X is the diffusion distance, D the diffusion coefficient, and t the time, with the total diffusion distance calculated by summing the diffusion distances in 1°C increments from the peak temperature to 300°C, with the cooling rate determining the time for each increment. The use of 300°C as the final temperature is arbitrary. However, the temperature used does not significantly affect the results, since most of the diffusion occurs near the peak temperature. The Fe-Mg diffusion coefficient in olivine depends on composition (BUENING and BUSECK, 1973; MISENER, 1974). In our simplified calculation, the fayalite concentration of olivine remains fixed throughout the cooling interval. We chose an average value of 15 mol% Fa for olivines in type IA chondrules in LL chondrites, which progress from Fa_{1-3} in LL3.0 to Fa_{30} in LL5. Calculations performed for Fa_{10} and Fa_{20} show that the modelling is relatively insensitive to this compositional parameter.

We have used the same expression as MIYAMOTO et al. (1986), given below, to extrapolate the experimental data of BUENING and BUSECK (1973) for the diffusion coefficient of Fe in olivine to low temperature:

$$D_{Fe} = 10^2(f_{O_2})^{1/6} \exp(-0.0501\ C_{Fe} - 14.03) \times \exp[(-31.66 + 0.2191\ C_{Fe})/RT] \quad (1)$$

where D_{Fe} is the Fe-Mg interdiffusion coefficient in $cm^2\ s^{-1}$, C_{Fe} is the mole % fayalite content of the olivine, R is the gas constant (1.987×10^{-3} Kcal K^{-1} mol^{-1}), and T is the temperature in Kelvin. This expression was derived for diffusion at temperatures between 1125 and 1000°C. The temperature dependence of the oxygen fugacity was calculated using the relationship determined by BRETT and SATO (1984) for LL chondrites:

$$\log(f_{O_2}) = 4.65 - 25800/T. \quad (2)$$

In contrast, our expression (Eqn. 3) for the diffusion coefficient using the data of MISENER (1974) (below) differs from the equation of MIYAMOTO et al. (1986) (Eqn. 4):

$$D_{Fe} = 10^2(f_{O_2})^{1/6}\ (0.0041 + 0.000112\ C_{Fe}) \times \exp[(-58.88 + 0.0905\ C_{Fe})/RT]. \quad (3)$$

The expression used by MIYAMOTO et al. (1986) is (M. MIYAMOTO, pers. comm., 1990):

$$D_{Fe} = (f_{O_2})^{1/6}\ (-3.4497 + 0.000112\ C_{Fe}) \times \exp[(-39.27 + 0.0905\ C_{Fe})/RT]. \quad (4)$$

The major differences between these expressions arise from the different methods used in incorporating the f_{O_2} term into the expression of MISENER (1974), who did not report a dependence on oxygen fugacity conditions for his experiments. Since D_{Fe} is dependent on oxygen fugacity, which is ultimately dependent on temperature, an oxygen fugacity correction must be applied. MIYAMOTO et al. (1986) formulated their version of MISENER (1974) for the specific case of the QFM buffer. Our expression uses the more general term $10^2 (f_{O_2})^{1/6}$ determined by BUENING and BUSECK (1973) for oxygen fugacity. Our expression yields diffusion coefficients similar to those measured by MISENER (1974) in the range of experimental temperatures.

Cooling from 520°C (the peak temperature for Parnallee) to 300°C at a rate of 10°C/Ma (the metallographic cooling rate of Parnallee) gives a total diffusion distance of approximately 4000 μm using the diffusion data of BUENING and BUSECK (1973) (Fig. 14a). Such a large diffusion distance would result in equilibrated olivines, inconsistent with zoned olivines observed in Parnallee. In sharp contrast, calculation using the data of MISENER (1974), as given in Eqn. (3) (Fig. 14b), results in approximately 35 μm of diffusion for the same temperature interval, consistent with observed diffusion distances in olivines of Parnallee (Fig. 3a).

The results obtained from olivine diffusion modelling are highly dependent on the version of the diffusion equation used. We estimate that at 500°C, the diffusion coefficients of BUENING and BUSECK (1973) and MISENER (1974) measured at high temperatures (1000–1125°C) may be in error by 10^2 and 10^3, respectively, based on extrapolations of one standard deviation error on the linear regression of the data. These errors can significantly affect any interpretation based on diffusion modelling. In the case of the BUENING and BUSECK (1973) data, the average diffusion distance in cooling from 520 to 300°C at 10°C/Ma could be as little as 400 μm. However, this is still significantly more diffusion than is observed in Parnallee. On the other hand, cooling through the same temperature interval could result in 1000 μm of diffusion using the data of MISENER (1974), when errors are considered. In summary, the diffusion data of BUENING and BUSECK (1973) cannot be used to model this low temperature

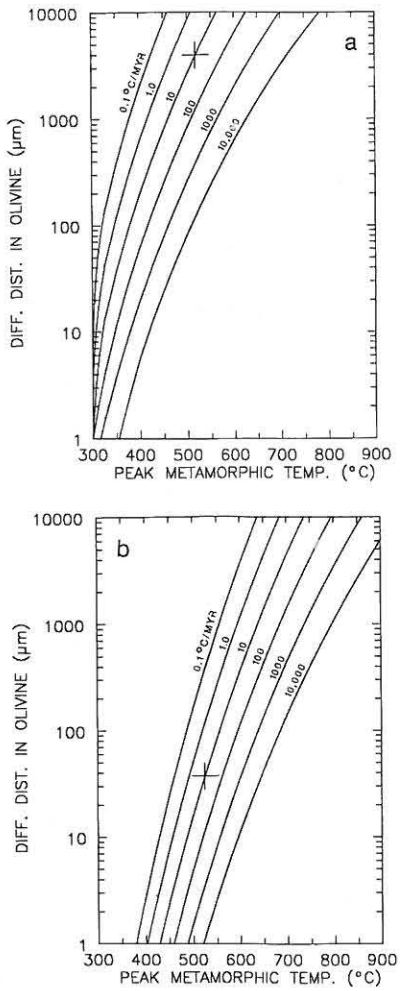

FIG. 14. Plots of average diffusion distance in olivine vs. peak metamorphic temperature for different cooling rates. Calculations used low temperature extrapolations of the diffusion data of (a) BUENING and BUSECK (1973) and (b) MISENER (1974). The cross represents Parnallee's metallographic cooling rate of 10°C/Ma and peak metamorphic temperature of at least 520°C. The curves in (a) give a diffusion distance of 4000 μm, while (b) gives 35 μm of diffusion. The latter are consistent with our observations.

diffusion, even when errors are considered, while the data of MISENER (1974) must be used with caution because of large possible uncertainties. More objectively, WILSON (1982) and OZAWA (1983, 1984) studied olivine-spinel zoning in terrestrial systems and concluded that the MISENER (1974) diffusion equation better reflects diffusion at low temperatures.

A generalized set of curves defining the temperatures and cooling rates at which olivines would be homogenized (i.e., defining the upper limit for cooling histories for type 3 chondrites) was derived by MIYAMOTO et al. (1986) (Fig. 15a). The solid lines were derived using the data of BUENING and BUSECK (1973) and the dashed lines those of MISENER (1974). The region labelled "Not Homogenized" (representing greater than 5% deviation from a uniform composition) is the area of interest for type 3 chondrites. Since most type 3 chondrites cooled between 1 and 10°C/Ma, a peak temperature of less than 400°C is indicated by the MISENER (1974) curves. This is inconsistent with metallographic peak temperature data from Parnallee.

We have used our calculations for average diffusion distance to produce a similar pair of curves (Fig. 15b). Our criterion for "Not Homogenized" in this work is a calculated average diffusion distance less than 100 μm, while homogenized olivines are those calculated to have diffusion distances greater than 1000 μm. Although different criteria are used, our curves calculated with the data of BUENING and BUSECK (1973) are similar to those of MIYAMOTO et al. (1986), in spite of our much simplified calculations. However, our curves for the data of MISENER (1974) are shifted to higher peak temperatures than those of MIYAMOTO et al. (1986),

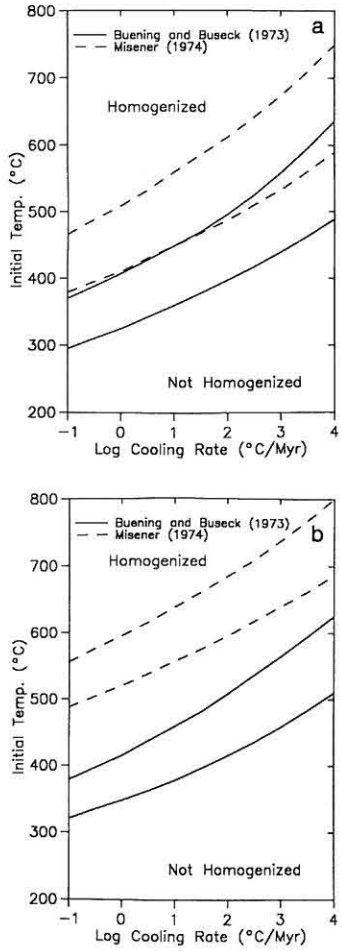

FIG. 15. Dependence of olivine homogenization on initial temperature (°C) and cooling rate (°C/Ma): (a) modelling of MIYAMOTO et al. (1986); (b) this work. Modelling of MIYAMOTO et al. (1986) indicates a peak metamorphic temperature of 400°C for type 3 chondrites that cooled between 1 and 10°C/Ma. This is inconsistent with the metallographic data for Parnallee (Fig. 13) and other type 3 ordinary chondrites which indicate peak metamorphic temperatures of at least 600°C for type 3 chondrites (MCCOY et al., 1990). Our modelling (b), which calculated average diffusion distances in olivine (see text), indicates peak temperatures of at least 525°C for type 3 chondrites. The agreement between our results and those of MIYAMOTO et al. (1986) for the diffusion data of BUENING and BUSECK (1973) indicates that our criteria for homogenization are in reasonable agreement with those of MIYAMOTO et al. (1986). Our results are consistent with thermal histories for type 3 chondrites.

consistent with the differences in diffusion expressions used. Our curves suggest that type 4–6 chondrites, with homogenized olivines, were heated above 600°C, while type 3 chondrites could have been heated to 525°C and retained grossly heterogeneous olivines. High petrologic type 3 chondrites, with partly homogenized olivines, could have been heated to between 525 and 600°C. These temperatures are more consistent with temperatures and cooling rates derived by Fe-Ni data, as well as the metamorphic temperatures estimated by DODD (1969).

The results of this modelling alone do not rule out the possibility that some diffusion occurred at higher temperatures for shorter periods of time, such as might be present in the solar nebula. For example, cooling at 10,000°C/Ma from 800°C would homogenize olivines in only 60,000 years (Fig. 15b), well within the one-million-year lifetime of the solar nebula. Nevertheless, the metallographic cooling rates demonstrate that chondrites cooled slowly in parent bodies. In the case of Parnallee, we can model the Fe-enrichments observed in type IA olivines as the result of the parent body thermal history alone. Additionally, the parent body thermal history of equilibrated chondrites would be sufficient to homogenize olivines (Fig. 15b). In other words, parent body metamorphism alone is sufficient to account for the Fe-Mg compositional trends described here. Nebular metasomatism is superfluous.

Minor element zoning in olivine

Using time scales indicated by metallographic cooling rates, we should also be able to model diffusion distances of minor elements in olivines. Diffusion rates of Ni, Co, Mn, and Ca have been measured by MORIOKA (1981). Calculations for the diffusion of these elements is considerably more complex than that of Fe-Mg. This complexity results from the initial zoning of some of these elements (MnO and CaO) and the decrease in concentrations (CaO). In light of these complexities, our simple diffusional modelling is probably unable to clarify the thermal regime in which such modification occurred. It is certain that secondary changes in MnO and CaO zoning and concentration (Fig. 3b and c) are less marked than those of FeO, and this observation is consistent with slower diffusion rates for these elements relative to iron.

Diffusion in pyroxenes

HUEBNER and NORD (1981) review diffusion data for major and minor elements in pyroxenes and estimate diffusion of Fe in high-Ca pyroxene to be 10^2–10^3 times slower than in olivines. Diffusion rates for low-Ca pyroxene are unknown, making it necessary to use those for high-Ca pyroxene. Type IA pyroxenes are modified from low, flat FeO profiles in Semarkona to smooth profiles with FeO enrichments at the grain edges in Parnallee (Fig. 8). A diffusion distance of about 6 μm can be inferred, based on the average distance at which FeO enrichment begins. This diffusion distance would be achieved if Fe-Mg diffusion in pyroxenes is approximately 200 times slower than in olivines. This result is obtained by modifying the diffusion coefficient in Eqn. (3) to obtain 6 μm of diffusion. This value falls within the range estimated by HUEBNER and NORD (1981). In summary, the zoning in type IA pyroxenes can be produced during parent body metamorphism using reasonable estimates for pyroxene diffusion rates.

Physical Setting

It is important to establish that chondrites on which these conclusions are based are composed of a single petrologic type, where chondrules and matrix were in direct contact during metamorphism. This assumption is confirmed by the narrow range of silicate compositions in a single chondrule type and coherent metallographic cooling rates shown by many of the chondrites studied, indicating a very similar thermal history for all components and a similar response to that thermal history. BINNS (1968) reports that Kelly and Soko-Banja are xenolithic; however, the arguments presented here are not based on these meteorites.

Our results do not allow us to distinguish between progressive metamorphism (heating of cold material) and autometamorphism (accretion of hot material at the peak metamorphic temperature), but other considerations argue against autometamorphism. WATANABE et al. (1985) argue for autometamorphism based on their transmission electron microscopy studies of spinodal decomposition in pyroxene. However, for autometamorphism, it is necessary to accrete hot material, around 1000 K, and bury it rapidly to depths of tens of kilometers (consistent with 1–10°C/Ma cooling rates) before significant cooling takes place. This required surprisingly prompt accretion after chondrule formation or high ambient nebular temperatures. Further arguments for autometamorphism were put forward by ASHWORTH et al. (1984), based on the results of annealing experiments on striated low-Ca pyroxenes. However, experiments carried out by BREARLEY and JONES (1988) have shown that the inferences drawn from these experiments may not be applicable to all chondrites, and that the microstructures of low-Ca pyroxenes are compatible with progressive metamorphism.

Evidence from our work indicates that the LL chondrite parent bodies were originally composed of material similar to that now preserved in Semarkona. Specifically, the porphyritic olivine chondrules now observed in metamorphosed chondrites were once similar to those now observed in the least equilibrated LL chondrite, Semarkona (LL3.0). Heating caused solid-state diffusive exchange between chondrules and matrix. This exchange is most evident in the increase in FeO in bulk chondrules and corresponding decrease in the fine-grained matrix, although many other elements record similar compositional trends. The formation of a compositional sequence was the result of varying degrees of metamorphism between chondrites, over a period of tens of millions of years. Additionally, subtle textural changes resulted because of this metamorphism. The compositional and textural changes are now reflected in the petrologic sequence of ordinary chondrites.

CONCLUSIONS

Several major conclusions can be drawn from this work. Although these conclusions are only strictly valid in the case of LL chondrites, it is likely that they apply to H and L chondrites as well.

1) Compositional data for olivines and low-Ca pyroxenes in types IA and II porphyritic olivine chondrules for LL3.0–5 chondrites define simple, monotonic trends. The processes acting on type 3 chondrites were not fundamentally different from those which affected type 4–6 chondrites.
2) Chemical data for silicates in LL3.3–5 chondrites indicate that porphyritic olivine chondrules in these chondrites can be derived from similar chondrules in the least metamorphosed LL chondrite, Semarkona (LL3.0).
3) The chemical trends defined by the minerals of type IA and type II chondrules can be satisfactorily accounted for by solid-state diffusive equilibration between minerals in chondrules and opaque matrix like those now preserved in Semarkona. We see no evidence that these chemical trends are due to changes in conditions during chondrule crystallization.
4) Metallographic cooling rates and radiometric ages are consistent with metamorphic time scales on the order of tens of millions of years. This is much longer than maximum time scales for the nebular lifetime, clearly showing that metamorphism occurred in asteroids or planetesimals. Some chemical modification in chondrule silicates could also have occurred at high temperatures in the solar nebula. However, diffusional modelling suggests that parent body metamorphism *alone* can account for chondrule silicate homogenization.

Acknowledgments—We would like to thank J. T. Wasson, A. E. Rubin, R. S. Clarke, Jr., and the Meteorite Working Group for kindly providing samples for this work. I. Casanova assisted with computer programming for the diffusion modelling calculations. T. Servilla, K. Nichols, and G. Conrad provided technical assistance for this work. Helpful discussions with M. Miyamoto and thorough reviews by R. Hewins, G. Huss, and an anonymous reviewer improved the manuscript. This study was funded in part by the National Aeronautics and Space Administration, Grants NAG 9-30 and 9-454 to Klaus Keil. One of us (TJM) was funded for travel by the Student Research Allocations Committee of the Graduate Student Association, University of New Mexico. This work was submitted by TJM in partial fulfillment of the requirements for the M.S. degree from the University of New Mexico. This is Planetary Geosciences Division Publication No. 625 and School of Ocean and Earth Science and Technology Publication No. 2387.

Editorial handling: E. J. Olsen

REFERENCES

ASHWORTH J. R., MALLINSON L. G., HUTCHISON R., and BIGGAR G. M. (1984) Chondrite thermal histories constrained by experimental annealing of Quenggouk orthopyroxene. *Nature* **308,** 259–261.

BENCE A. E. and ALBEE A. L. (1968) Empirical correction factors for the microanalysis of silicates and oxides. *J. Geol.* **76,** 382–403.

BINNS R. A. (1968) Cognate xenoliths in chondritic meteorites: Examples in Mezö-Madaras and Ghubara. *Geochim. Cosmochim. Acta* **32,** 299–317.

BREARLEY A. J. (1990) Carbon-rich aggregates in type 3 ordinary chondrites: Characterization, origins, and thermal history. *Geochim. Cosmochim. Acta* **54,** 831–850.

BREARLEY A. J. and JONES R. H. (1988) An experimental investigation of the ortho/clino transition in low-Ca pyroxenes and its application to thermal histories of chondritic meteorites (abstr.) *Eos* **69,** 1506.

BRETT R. and SATO M. (1984) Intrinsic oxygen fugacity measurements on seven chondrites, a pallasite, and a tektite and the redox state of meteorite parent bodies. *Geochim. Cosmochim. Acta* **48,** 111–120.

BUENING D. K. and BUSECK P. R. (1973) Fe-Mg lattice diffusion in olivine. *J. Geophys. Res.* **78,** 6852–6862.

CASANOVA I., KEIL K., WIELER R., SAN MIGUEL A., and KING E. A. (1990) Origin and history of regolith, fragmental and impact-melt breccias from Spain. *Meteoritics* **25,** 127–136.

DODD R. T., JR. (1969) Metamorphism of the ordinary chondrites: a review. *Geochim. Cosmochim. Acta* **33,** 161–203.

DODD R. T., JR., VAN SCHMUS W. R., and KOFFMAN D. M. (1967) A survey of the unequilibrated ordinary chondrites. *Geochim. Cosmochim. Acta* **31,** 921–951.

DONALDSON C. H. (1976) An experimental investigation of olivine morphology. *Contrib. Mineral. Petrol.* **57,** 187–213.

FREDRIKSSON K. (1983) Crystallinity, recrystallization, equilibration, and metamorphism in chondrites. In *Chondrules and Their Origins* (ed. E. A. KING), pp. 44–52. Lunar and Planetary Science Institute, Houston.

GOMES C. B. and KEIL K. (1980) *Brazilian Stone Meteorites.* Univ. New Mexico Press.

GRAHAM A. L., BEVAN A. W. R., and HUTCHISON R. (1985) *Catalogue of Meteorites.* Univ. Arizona Press.

GROSSMAN J. N. (1988) Formation of chondrules. In *Meteorites and the Early Solar System* (eds. J. F. KERRIDGE and M. S. MATTHEWS), pp. 680–696. Univ. Arizona Press.

GUIMON R. K., LOFGREN G. E., and SEARS D. W. G. (1988) Chemical and physical studies of type 3 chondrites. IX: Thermoluminescence and hydrothermal annealing experiments and their relationship to metamorphism and aqueous alteration of type <3.3 ordinary chondrites. *Geochim. Cosmochim. Acta* **52,** 119–127.

HEWINS R. H. (1989) The evolution of chondrules. *Proc. NIPR Symp. Antarctic Meteorites* **2,** 200–220. National Institute of Polar Research, Tokyo.

HEWINS, R. H. (1990) Chondrule evolution revisited: Semarkona and Chainpur (abstr.). *Lunar Planet. Sci. Conf.* **XXI,** 507–508.

HEYSE J. V. (1978) The metamorphic history of LL-group chondrites. *Earth Planet. Sci. Lett.* **40,** 365–381.

HUA X., ADAM J., PALME H., and EL GORESEY A. (1988) Fayalite-rich rims, veins, and haloes around and in forsterite olivines in CAIs and chondrules in carbonaceous chondrites: Types, compositional profiles and constraints on their formation. *Geochim. Cosmochim. Acta* **52,** 1389–1408.

HUEBNER J. S. and NORD G. L., JR. (1981) Assessment of diffusion in pyroxenes: What we do and do not know (abstr.). *Lunar Planet. Sci. Conf.* **XII,** 479–481.

HUSS G. R., KEIL K., and TAYLOR G. J. (1981) The matrices of unequilibrated ordinary chondrites: implications for the origin and history of chondrites. *Geochim. Cosmochim. Acta* **45,** 33–51.

JOHNSON M. C. (1986) The solar nebula redox state as recorded by the most reduced chondrules of five primitive chondrites. *Geochim. Cosmochim. Acta* **50,** 1497–1502.

JONES R. H. (1990) Petrology and mineralogy of type II, FeO-rich chondrules in Semarkona (LL3.0): Origin by closed system fractional crystallization, with evidence for supercooling. *Geochim. Cosmochim. Acta* **54,** 1785–1802.

JONES R. H. and RUBIE D. C. (1990) Thermal metamorphism in CO3 chondrites: Application of olivine diffusion modelling to post-accretionary metamorphism (abstr.) *Lunar. Planet. Sci.* **XXI,** 583–584.

JONES R. H. and SCOTT E. R. D. (1989) Petrology and thermal history of type IA chondrules in the Semarkona (LL3.0) chondrite. *Proc. 19th Lunar Planet. Sci. Conf.,* 523–536.

KEIL K. (1962) On the phase composition of meteorites. *J. Geophys. Res.* **67,** 4055–4061.

KRING D. A. (1985) Heterogeneity of O/H in the solar nebula, as indicated by mafic mineral compositions in chondrules (abstr.). *Lunar Planet. Sci. Conf.* **XV.** 469–470.

KURAT G. (1988) Primitive meteorites: an attempt towards unification. *Phil. Trans. Roy. Soc. London* **A325,** 459–482.

LUX G., KEIL K., and TAYLOR G. J. (1980) Metamorphism of the H-group chondrites: Implications from compositional and textural trends in chondrules. *Geochim. Cosmochim. Acta* **44,** 841–855.

MCCOY T. J. (1990) Metamorphism, brecciation and parent body structures of LL-group chondrites. M.S. thesis, Univ. New Mexico.

McCoy T. J., Taylor G. J., Scott E. R. D., and Keil K. (1990) Metallographic cooling rates correlated with petrologic type in LL3.0–4 chondrites: Implications for parent body structures (abstr.). *Lunar Planet. Sci. Conf.* **XXI,** 749–750.

McSween H. Y., Jr. (1977) On the nature and origin of isolated olivine grains in carbonaceous chondrites. *Geochim. Cosmochim. Acta* **41,** 411–418.

McSween H. Y., Jr., Sears D. W. G., and Dodd R. T. (1988) Thermal metamorphism. In *Meteorites and the Early Solar System* (eds. J. F. Kerridge and M. S. Matthews), pp. 102–113. Univ. Arizona Press.

Misener D. J. (1974) Cationic diffusion in olivine to 1400°C and 35 Kbar. *Geochemical Transport and Kinetics, Publ. 634,* pp. 117–129. Carnegie Institute, Washington, DC.

Miyamoto M., McKay D. S., McKay G. A. and Duke M. B. (1986) Chemical zoning and homogenization of olivines in ordinary chondrites and implications for thermal histories of chondrules. *J. Geophys. Res.* **91,** 12804–12816.

Morioka M. (1981) Cation diffusion in olivine—II. Ni-Mg, Mn-Mg, Mg and Ca. *Geochim. Cosmochim. Acta* **45,** 1573–1580.

Ozawa K. (1983) Evaluation of olivine-spinel geothermometry as an indicator of thermal history for peridotites. *Contrib. Mineral. Petrol.* **82,** 52–65.

Ozawa K. (1984) Olivine-spinel geospeedometry: analysis of diffusion-controlled Mg-Fe^{2+} exchange. *Geochim. Cosmochim. Acta* **48,** 2597–2611.

Palme H. and Fegley B., Jr. (1987) Formation of FeO-bearing olivine in carbonaceous chondrites by high temperature oxidation in the solar nebula (abstr.). *Lunar Planet. Sci. Conf.* **XVIII,** 754–755.

Palme H. and Fegley B., Jr. (1991) High temperature condensation of iron-rich olivine in the solar nebula. *Earth Planet. Sci. Lett.* (submitted).

Peck J. A. and Wood J. A. (1987) The origin of ferrous zoning in Allende chondrule olivines. *Geochim. Cosmochim. Acta* **51,** 1503–1510.

Pellas P. and Storzer D. (1981) ^{244}Pu fission track thermometry and its application to stony meteorites. *Proc. Roy. Soc. London* **A374,** 253–270.

Reid A. M. and Fredriksson K. (1967) Chondrules and chondrites. In *Researches in Geochemistry* (ed. P. H. Abelson), pp. 170–203. J. Wiley & Sons.

Scott E. R. D. (1984) Classification, metamorphism and brecciation of type 3 chondrites from Antarctica. *Smithsonian Contrib. Earth Sci.* **26,** 73–94.

Scott E. R. D. and Jones R. H. (1990) Disentangling nebular and asteroidal features of CO3 carbonaceous chondrite meteorites. *Geochim. Cosmochim. Acta* **54,** 2485–2502.

Scott E. R. D. and Taylor G. J. (1983) Chondrules and other components in C, O, and E chondrites: Similarities in their properties and origins. *Proc. 14th Lunar Planet. Sci. Conf.,* B275–B286.

Scott E. R. D., Taylor G. J., and Keil K. (1983) Type 3 ordinary chondrites—metamorphism, brecciation and parent bodies (abstr.). *Meteoritics* **18,** 393–394.

Scott E. R. D., Lusby D., and Keil K. (1985) Ubiquitous brecciation after metamorphism in equilibrated ordinary chondrites. *Proc. 16th Lunar Planet. Sci. Conf.; J. Geophys. Res.* **90,** D137–D148.

Scott E. R. D., Taylor G. J., and Keil K. (1986) Accretion, metamorphism, and brecciation of ordinary chondrites: evidence from petrologic studies of meteorites from Roosevelt County, New Mexico. *Proc. 17th Lunar Planet. Sci. Conf.; J. Geophys. Res.* **91,** E115–E123.

Sears D. W. G. and Hasan F. A. (1987) The type three ordinary chondrites: a review. *Surv. Geophys.* **9,** 43–97.

Taylor G. J., Scott E. R. D., and Keil K. (1983) Cosmic setting for chondrule formation. In *Chondrules and Their Origins* (ed. E. A. King), pp. 262–278. Lunar and Planetary Institute, Houston.

Tsuchiyama A., Fujita T., and Morimoto N. (1988) Fe-Mg heterogeneity in the low-Ca pyroxenes during metamorphism of the ordinary chondrites. *Proc. NIPR Symp. Antarctic Meteorites* **1,** 173–184.

Turner G., Enright M. C., and Cadogan P. H. (1978) The early history of chondrite parent bodies inferred from ^{40}Ar-^{39}Ar ages. *Proc. 9th Lunar Planet. Sci. Conf.,* 989–1025.

Van Schmus W. R. and Wood J. A. (1967) A chemical-petrologic classification for the chondritic meteorites. *Geochim. Cosmochim. Acta* **31,** 747–765.

Watanabe S., Kitamura M., and Morimoto N. (1985) A transmission electron microscope study of pyroxene chondrules in equilibrated L-group chondrites. *Earth Planet. Sci. Lett.* **72,** 87–98.

Willis J. and Goldstein J. I. (1981a) A revision of metallographic cooling rate curves for chondrites. *Proc. 12th Lunar Planet. Sci. Conf.,* 1135–1143.

Willis J. and Goldstein J. I. (1981b) Solidification zoning and metallographic cooling rates of chondrites. *Nature* **293,** 126–127.

Willis J. and Goldstein J. I. (1983) A three-dimensional study of metal grains in equilibrated, ordinary chondrites. *Proc. 14th Lunar Planet. Sci. Conf.,* B287–B292.

Wilson A. H. (1982) The geology of the Great 'Dyke', Zimbabwe: The ultramafic rocks. *J. Petrol.* **23,** 240–292.

Wood J. A. (1967) Chondrites: Their metallic minerals, thermal histories, and parent planets. *Icarus* **6,** 1–49.

Wood J. A. and Morfill G. E. (1988) A review of solar nebula models. In *Meteorites and the Early Solar System* (eds. J. F. Kerridge and M. S. Matthews), pp. 329–347. Univ. Arizona Press.